

SUPPORTING INFORMATION

Discovery and Characterization of XY101, a Potent, Selective, and Orally Bioavailable ROR γ Inverse Agonist for Treatment of Castration-Resistant Prostate Cancer (CRPC)

Yan Zhang,^{†,‡,§,¶} Xishan Wu,^{†,‡,§,¶} Xiaoqian Xue,^{†,||,¶} Chenchang Li,[†] Junjian Wang,^{⊥,∇} Rui Wang,[†] Cheng Zhang,^{†,○} Chao Wang,^{†,‡,§} Yudan Shi,^{†,‡,§} Lingjiao Zou,^{†,‡,§} Qiu Li,^{†,‡,§} Zenghong Huang,[∇] Xiaojuan Hao,[◆] Kerry Loomes,[¶] Donghai Wu,[&] Hong-Wu Chen,^{∇•} Jinxin Xu,[&] and Yong Xu^{*,†,§}

[†]Guangdong Provincial Key Laboratory of Biocomputing, Joint School of Life Sciences, Guangzhou Institutes of Biomedicine and Health, Chinese Academy of Sciences; Guangzhou Medical University, Guangzhou 510530, China.

[‡]University of Chinese Academy of Sciences, No. 19 Yuquan Road, Beijing 100049, China.

[§]Guangzhou Regenerative Medicine and Health Guangdong Laboratory (GRMH-GDL), Guangzhou 510530, China

^{||}School of Life Science, Huizhou University, Huizhou 516007, China

[⊥]School of Pharmaceutical Sciences, Sun Yat-Sen University, Guangzhou, 510006, China.

[∇]Department of Biochemistry and Molecular Medicine, School of Medicine, University of California, Davis, Sacramento, California 95817, USA.

[○]School of Pharmaceutical Sciences, Jilin University, Changchun, China, No.1266

Fujin Road, Chaoyang District, Changchun, Jilin 130021, China.

*Manufacturing, Commonwealth Scientific and Industrial Research Organization (CSIRO), Clayton, Vic 3168, Australia.

[†]School of Biological Sciences & Maurice Wilkins Centre, University of Auckland, Auckland 1010, New Zealand.

[&]Guangzhou Institutes of Biomedicine and Health, Chinese Academy of Sciences; Guangzhou 510530, China

^{*}UC Davis Comprehensive Cancer Center, University of California, Davis, Sacramento, California 95817, USA.

^{*}Corresponding Author: Yong Xu, PhD, E-mail: xu_yong@gibh.ac.cn

[#]These authors contributed equally to this work.

Table of Contents:

- 1. Table S1.** Statistics of the data sets and structure refinement.
- 2. Figure S1.** (A) The co-crystal structure of compound **27** in complex with the ROR γ LDB. (B) Superimposition of 3 complex structures from the asymmetry unit.
- 3. Figure S2.** (A) Superposition of the crystal structures of **27** and GSK-8h bound to ROR γ LBD (PDB IDs: 6JIL and 5NU1). (B) Superposition of the crystal structures of **27** and **1** bound to ROR γ LBD (PDB IDs: 6JIL and 5NTQ).
- 4. Figure S3.** ITC titration curves for the binding of **23** (A), **26** (B) and **27** (C) to the ROR γ LBD. Corresponding parameters were listed.
- 5. Figure S4.** Metabolic stability of **23**, **26**, **27** in rat liver microsome at 10 μ M.
- 6.** ^1H and ^{13}C NMR spectra of compounds **11-36**.

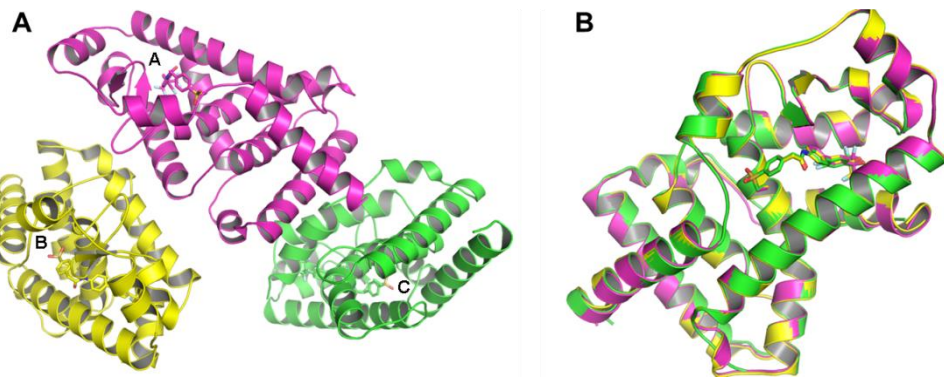
1. Table S1. Statistics of the data sets and structure refinement.

Protein/ligand	ROR γ /27
PDB ID:	6J1L.pdb
Space group	P6 ₁
Cell dimensions a, b, c (Å)	110.14, 110.14, 114.23
Cell dimensions α, β, γ (°)	90.00, 90.00, 120.00
Resolution (Å)*	2.30 (2.38-2.30)
R_{merge} *	0.108 (2.015)
I/σI*	13.2 (2.2)
Completeness (%)*	100 (100)
Redundancy	18.9 (18.6)
$R_{\text{work}}/R_{\text{free}}$	0.202/0.226
No. of atoms (P/L/O)	5424/114/71
B_f (P/L/O) (Å ²)	66.97/59.59/48.58
rms deviation bond(Å)	0.015
rms deviation angle (°)	1.704

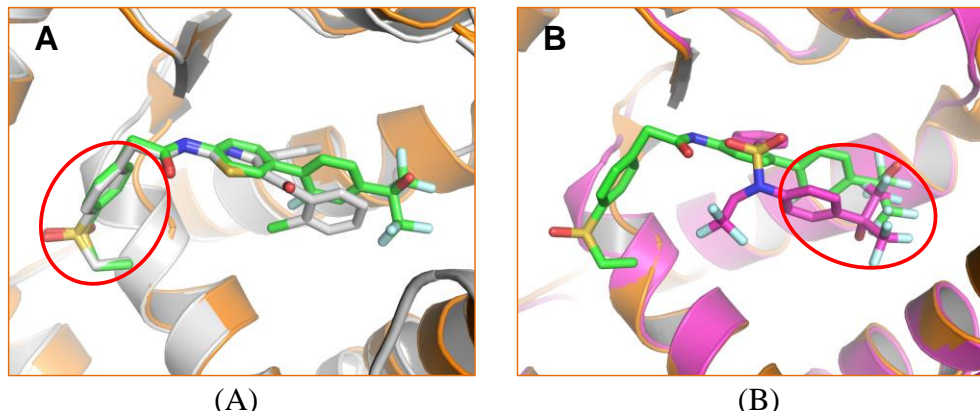
*Values in brackets show the statistics for the highest resolution shells.

^a P/L/O indicate protein, ligand, and other (water and other molecules), respectively.

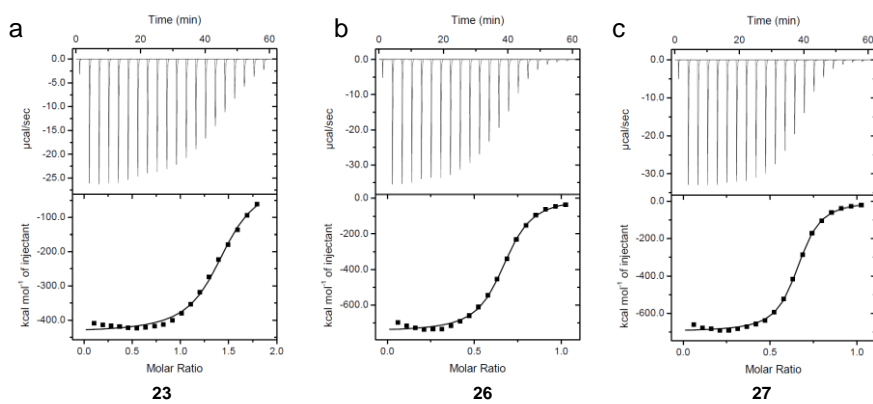
2. Figure S1. (A) The co-crystal structure of compound **27** in complex with the ROR γ LDB. (B) Superimposition of 3 complex structures from the asymmetry unit.



3. Figure S2. (A) Superposition of the crystal structures of **27** and GSK-8h bound to ROR γ LBD (PDB IDs: 6JIL and 5NU1). (B) Superposition of the crystal structures of **27** and **1** bound to ROR γ LBD (PDB IDs: 6JIL and 5NTQ).

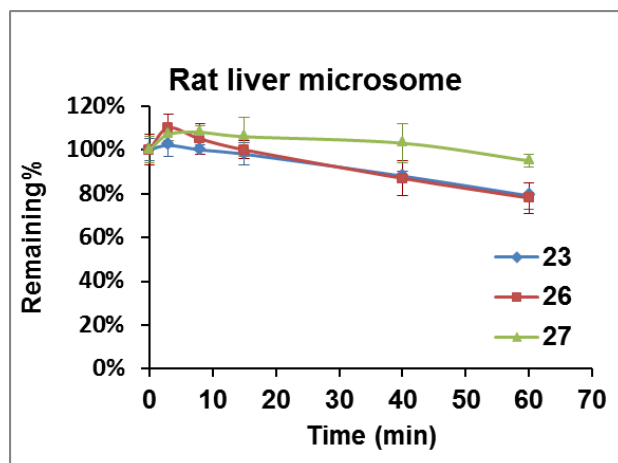


4. Figure S3. ITC titration curves for the binding of **23** (A), **26** (B) and **27** (C) to the ROR γ LBD. Corresponding parameters were listed.



Cmpd	Protein	N	K _D (nM)	ΔH (kcal/mol)	TΔS (kcal/mol)	ΔG (kcal/mol)
23	ROR γ	0.994 ± 0.006	781	-418.1 ± 3.6	-408.3	-9.8
26	ROR γ	1.020 ± 0.006	564	-734.1 ± 5.7	-724.1	-10.0
27	ROR γ	1.040 ± 0.004	380	-672.3 ± 3.6	-661.6	-10.7

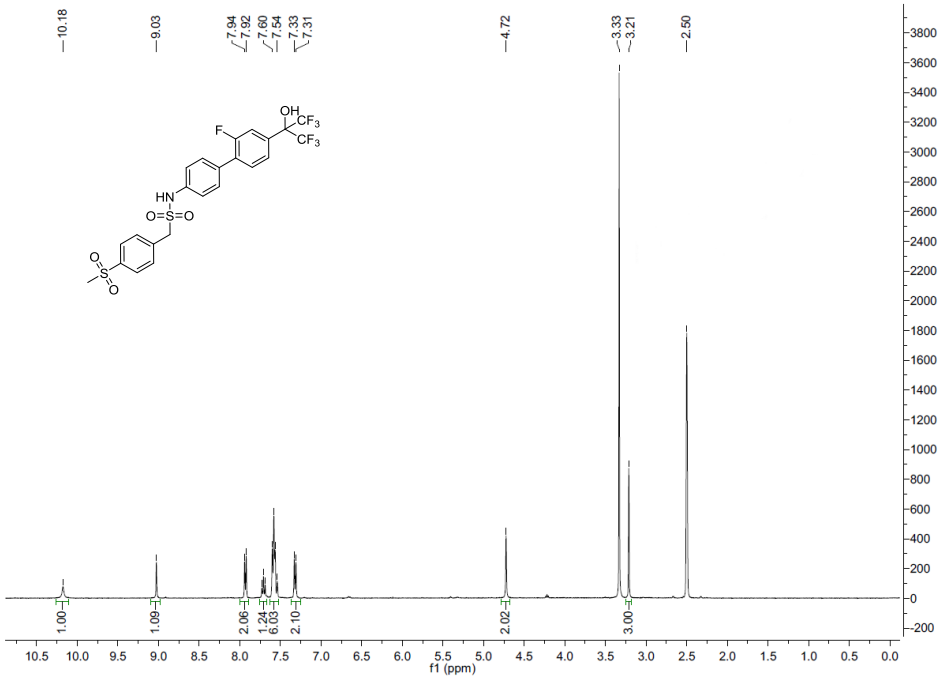
5. Figure S4. Metabolic stability of **23**, **26**, **27** in rat liver microsome at 10 μ M.



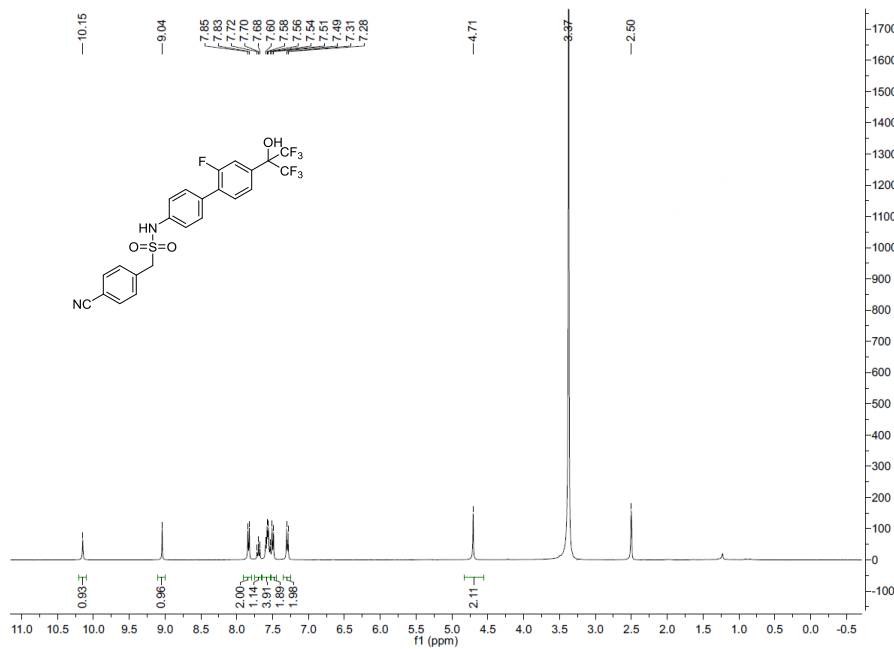
Cmpd	k	% of parent remaining after 1 h	T1/2 (min)
Testerone	-	26% (at 20 min)	-
23	0.00343	79%	202
26	0.00348	78%	199
27	0.00008	93%	>> 60

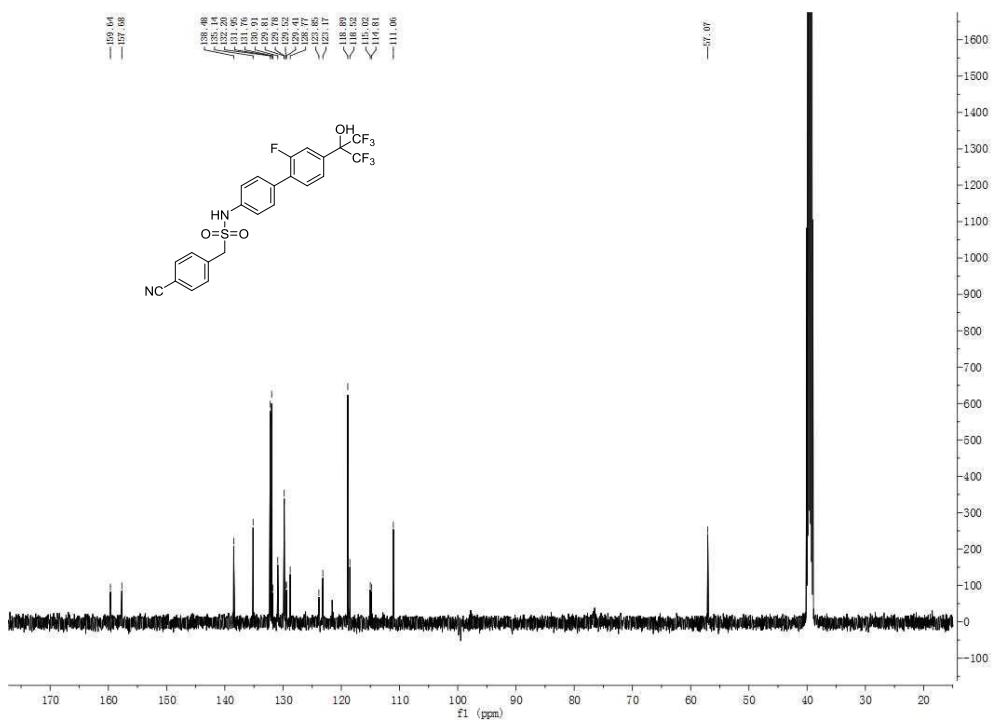
6. ^1H and ^{13}C NMR spectra of compounds 11-36.

N-(2'-fluoro-4'-(1,1,1,3,3,3-hexafluoro-2-hydroxypropan-2-yl)-[1,1'-biphenyl]-4-yl)-1-(4-(methylsulfonyl)phenyl)methanesulfonamide (**II**).

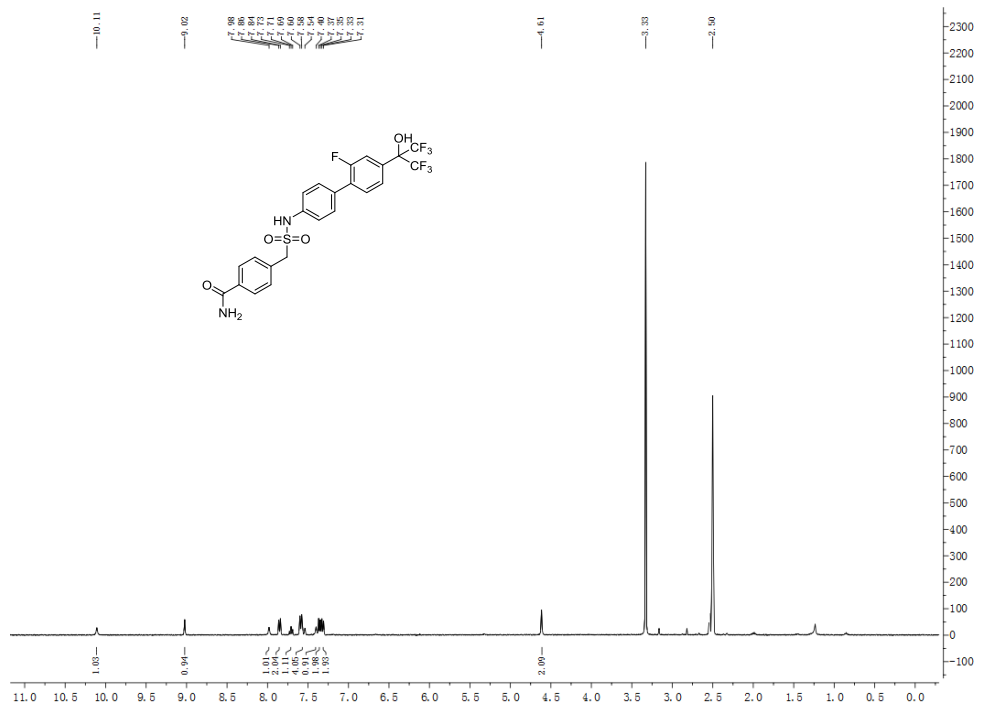


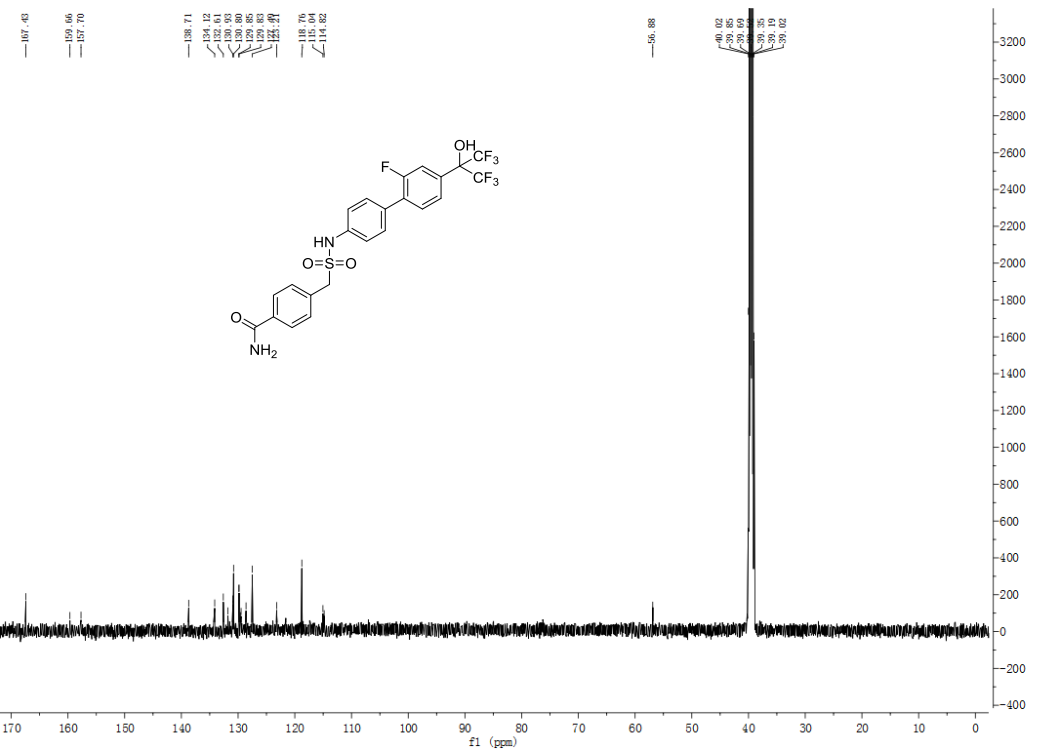
1-(4-cyanophenyl)-N-(2'-fluoro-4'-(1,1,1,3,3,3-hexafluoro-2-hydroxypropan-2-yl)-[1,1'-biphenyl]-4-yl)methanesulfonamide (12).



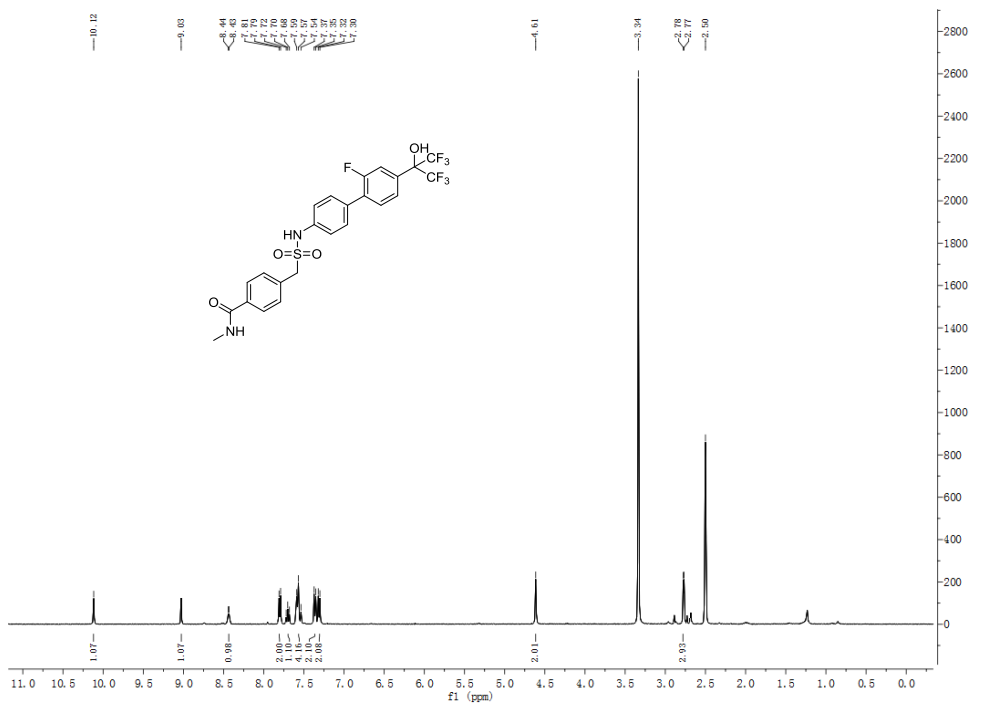


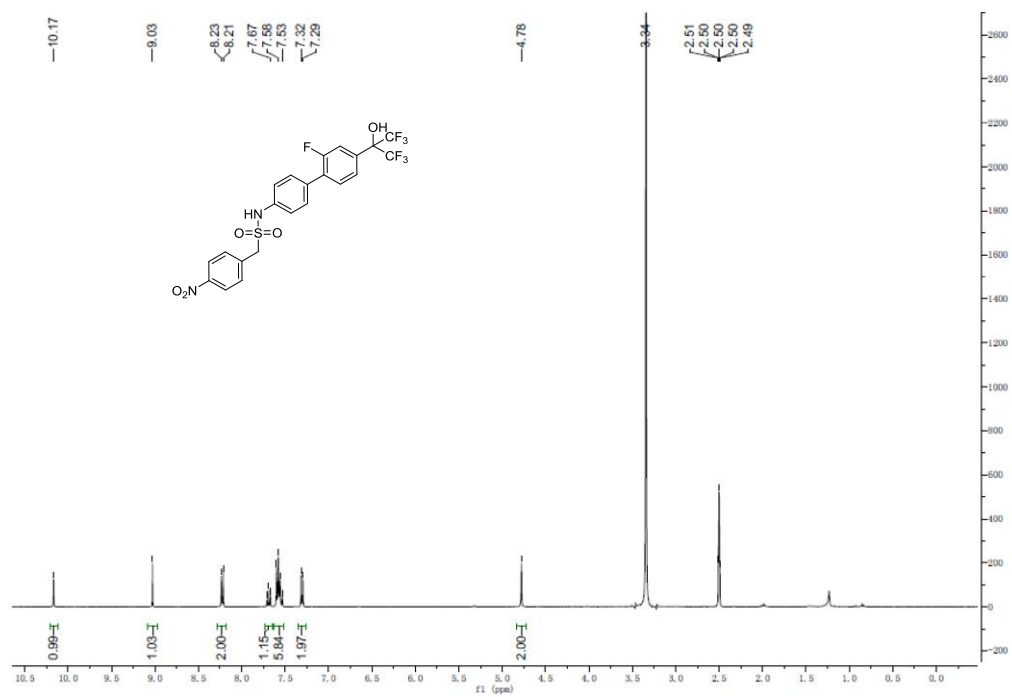
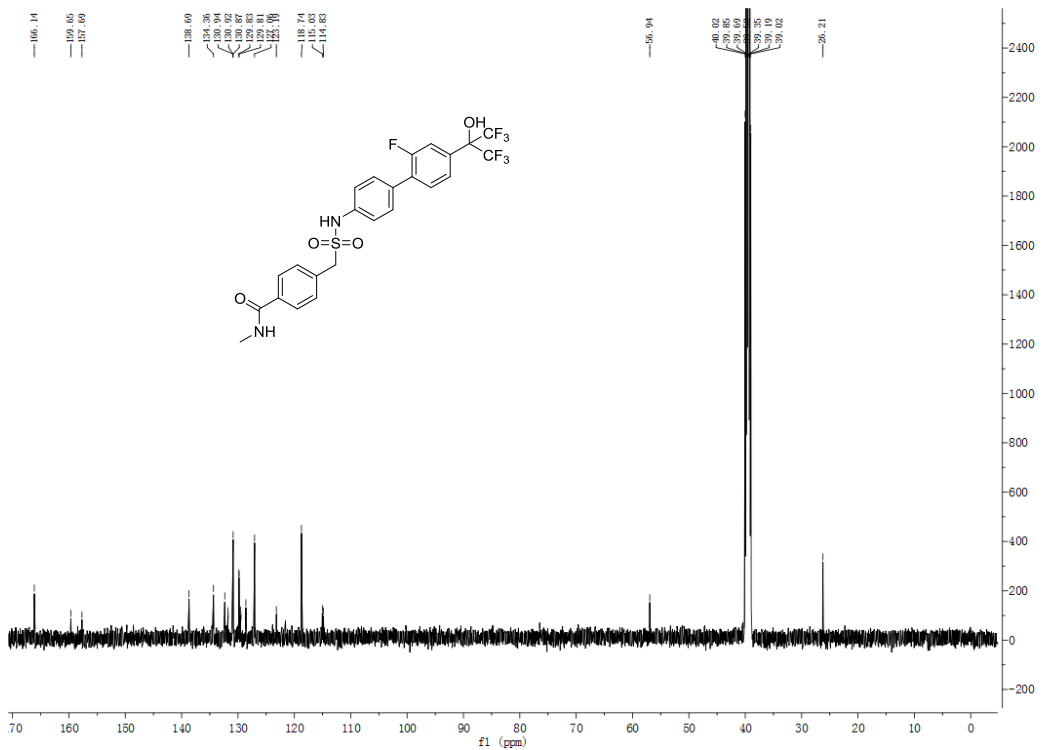
4-((N-(2'-fluoro-4'-(1,1,1,3,3,3-hexafluoro-2-hydroxypropan-2-yl)-[1,1'-biphenyl]-4-yl)sulfamoyl)methyl)benzamide (13).



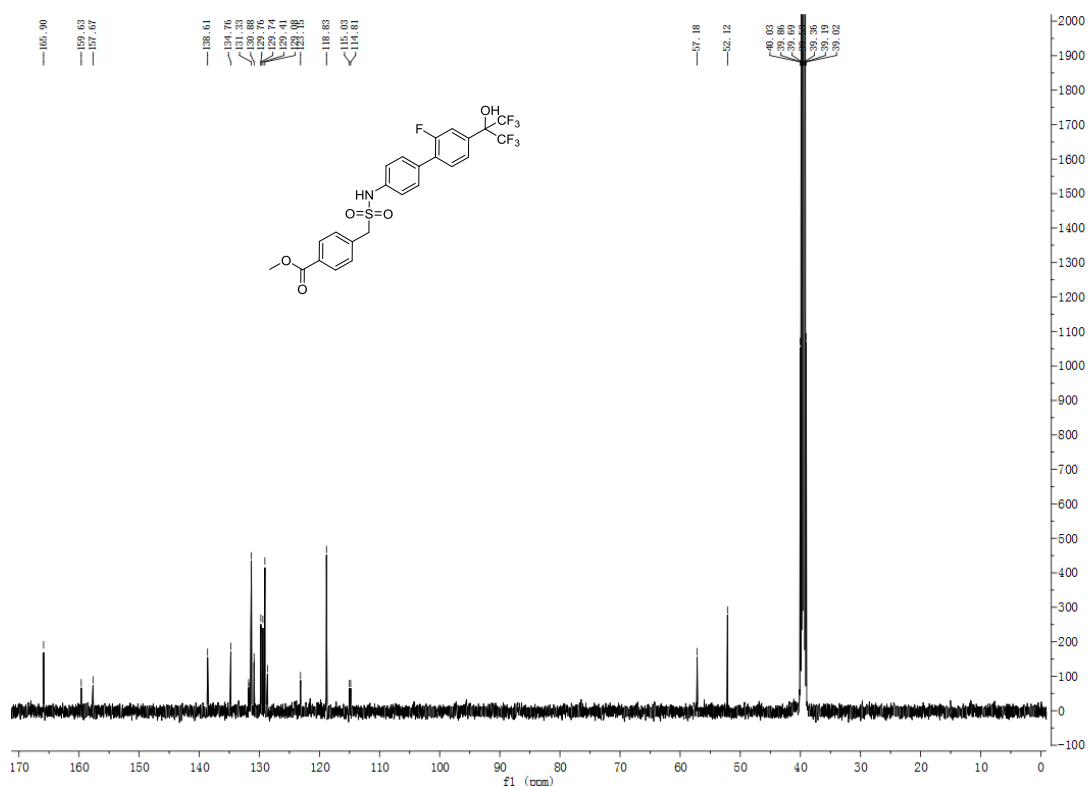
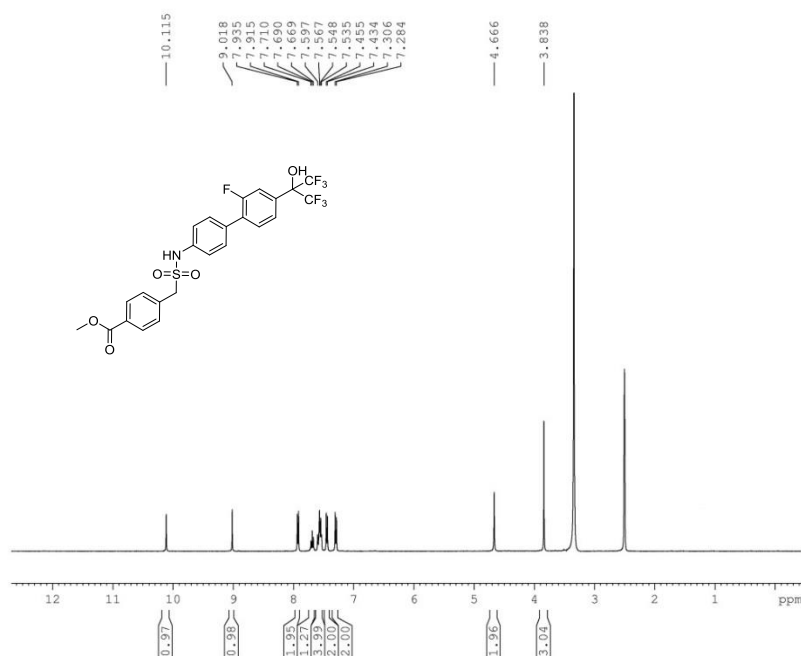


4-((N-(2'-fluoro-4'-(1,1,1,3,3,3-hexafluoro-2-hydroxypropan-2-yl)-[1,1'-biphenyl]-4-yl)sulfamoyl)methyl)-N-methylbenzamide (14).

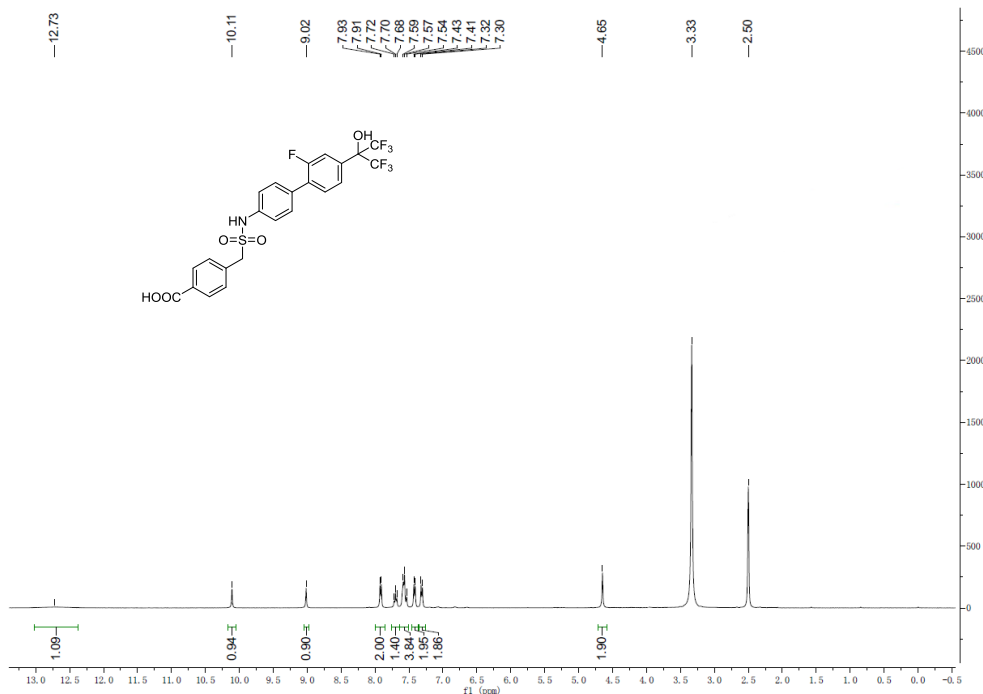




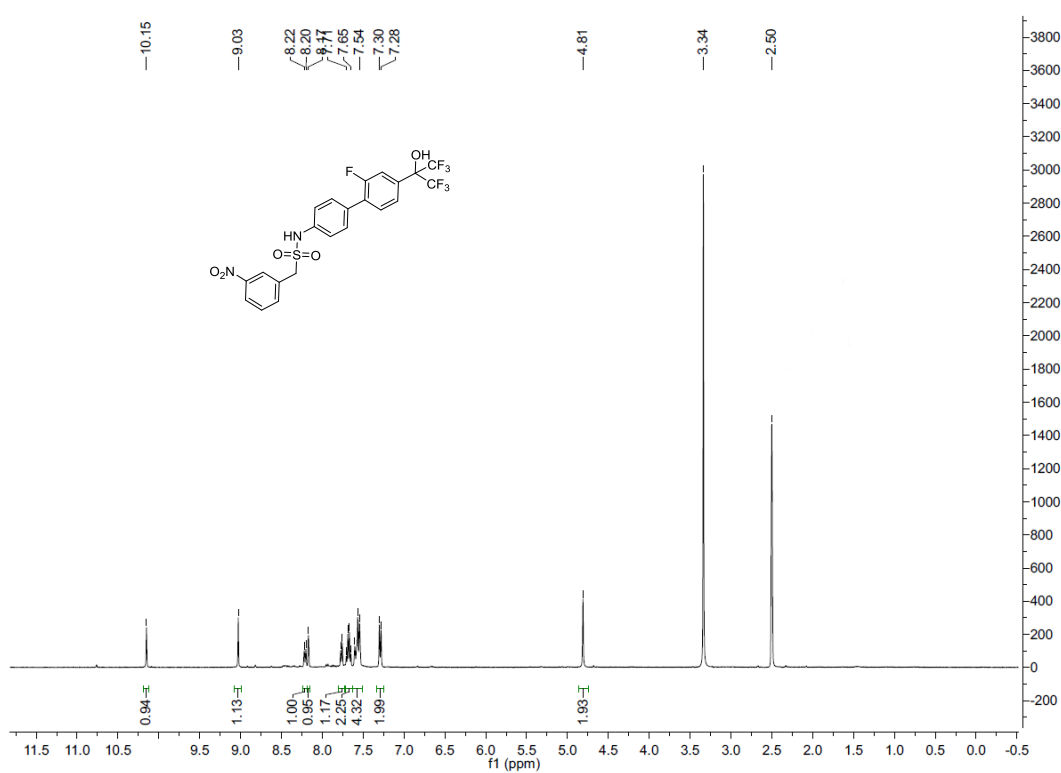
Methyl-4-((N-(2'-fluoro-4'-(1,1,1,3,3,3-hexafluoro-2-hydroxypropan-2-yl)-[1,1'-biphenyl]-4-yl)sulfamoyl)methyl)benzoate (16).

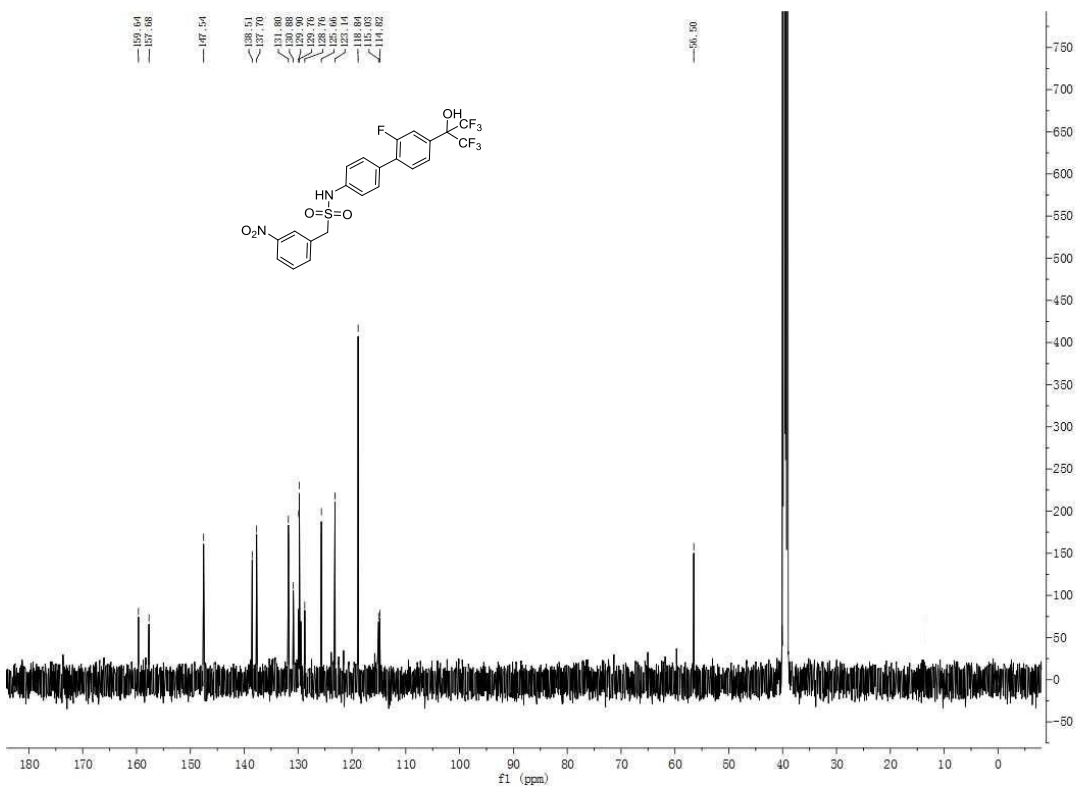


*4-((N-(2'-fluoro-4'-(1,1,1,3,3-hexafluoro-2-hydroxypropan-2-yl)-[1,1'-biphenyl]-4-yl)sulfamoyl)methyl)benzoic acid (**17**).*

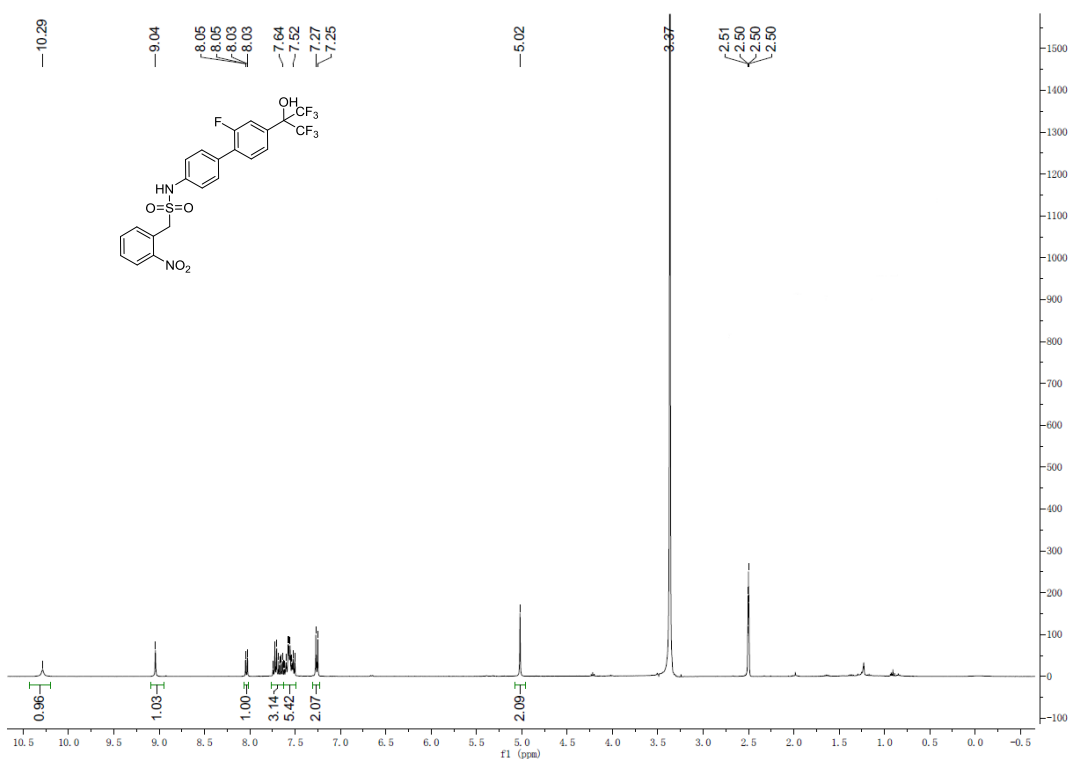


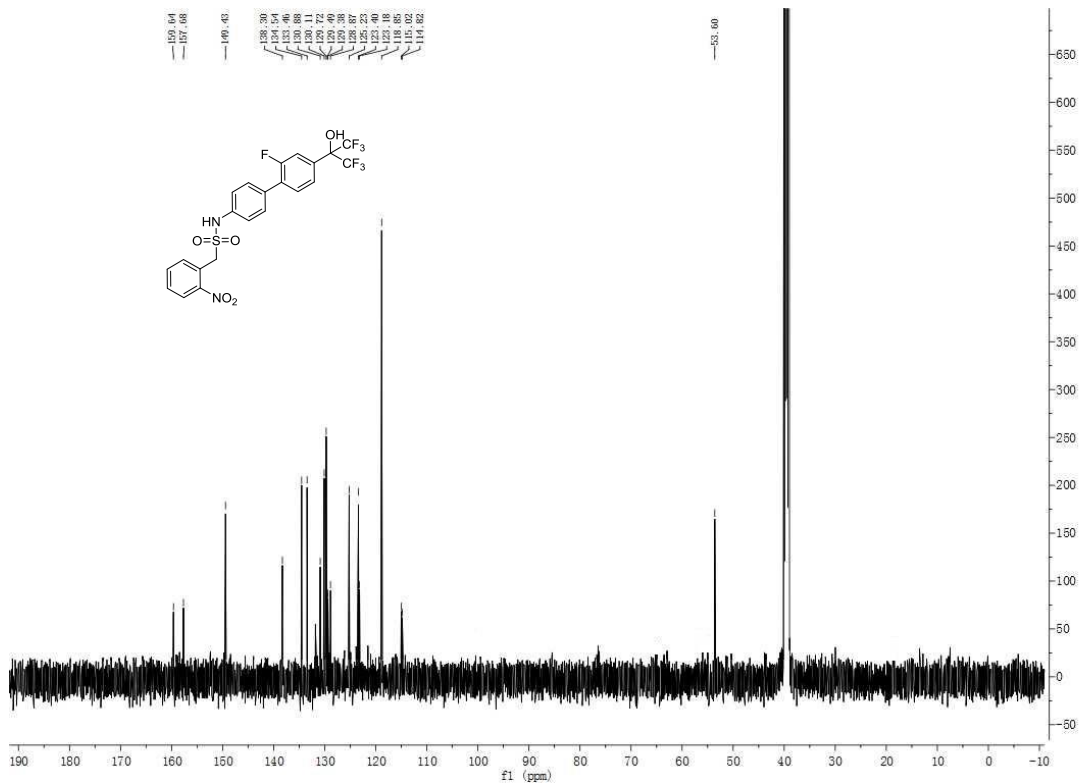
*N-(2'-fluoro-4'-(1,1,1,3,3-hexafluoro-2-hydroxypropan-2-yl)-[1,1'-biphenyl]-4-yl)-1-(3-nitrophenyl)methanesulfonamide (**18**).*



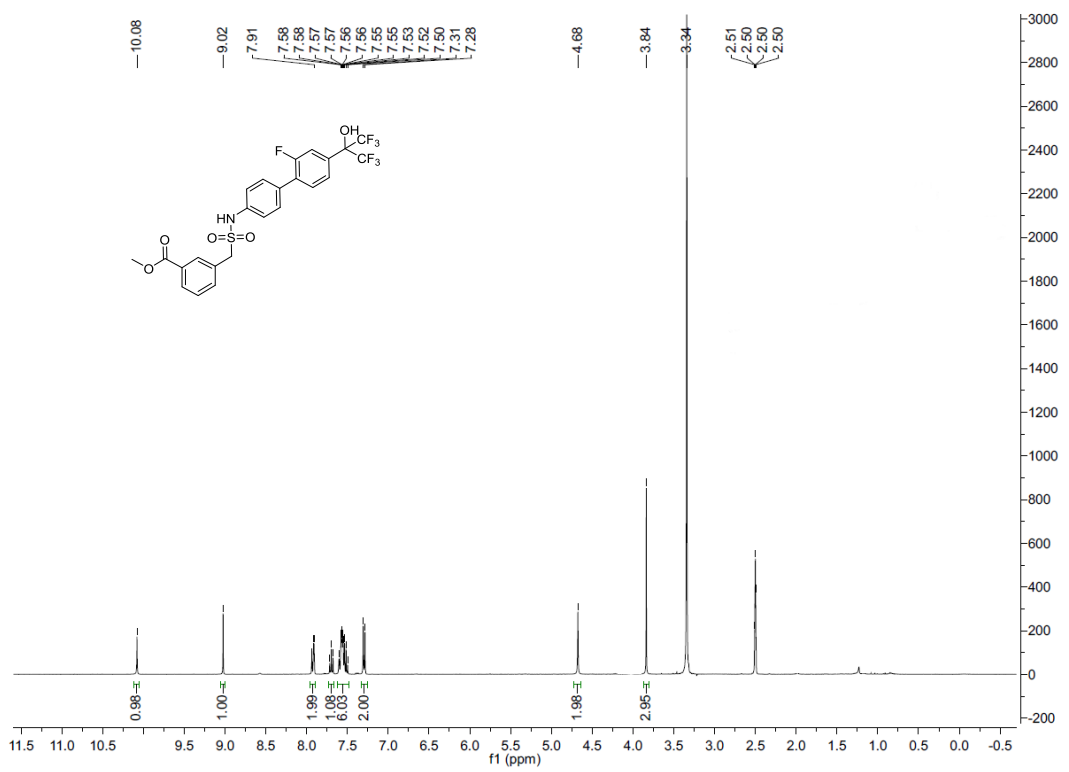


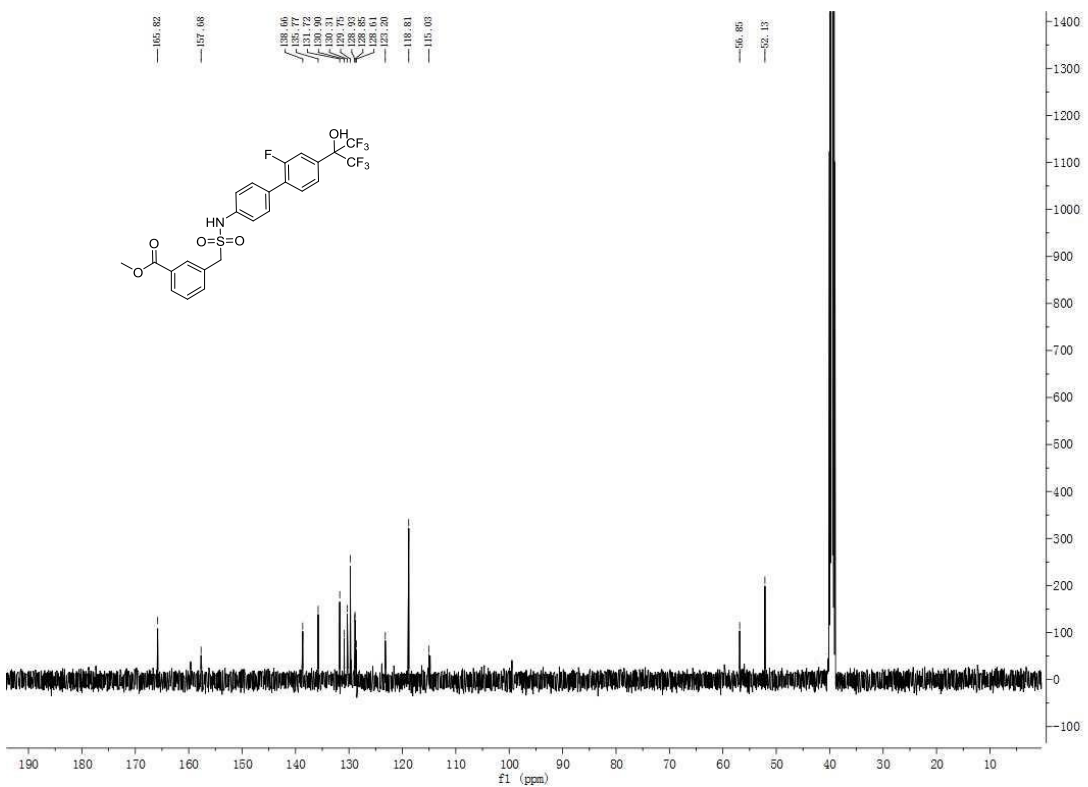
N-(2'-fluoro-4'-(1,1,1,3,3-hexafluoro-2-hydroxypropan-2-yl)-[1,1'-biphenyl]-4-yl)-1-(2-nitrophenyl) methanesulfonamide (**19**)



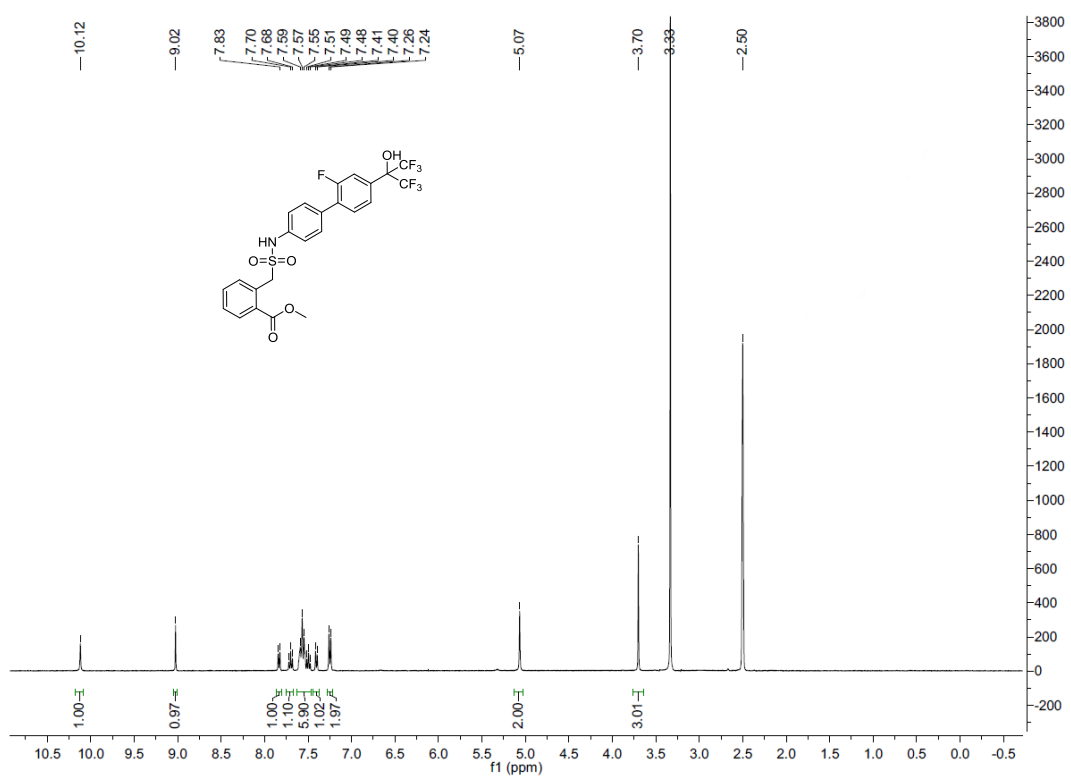


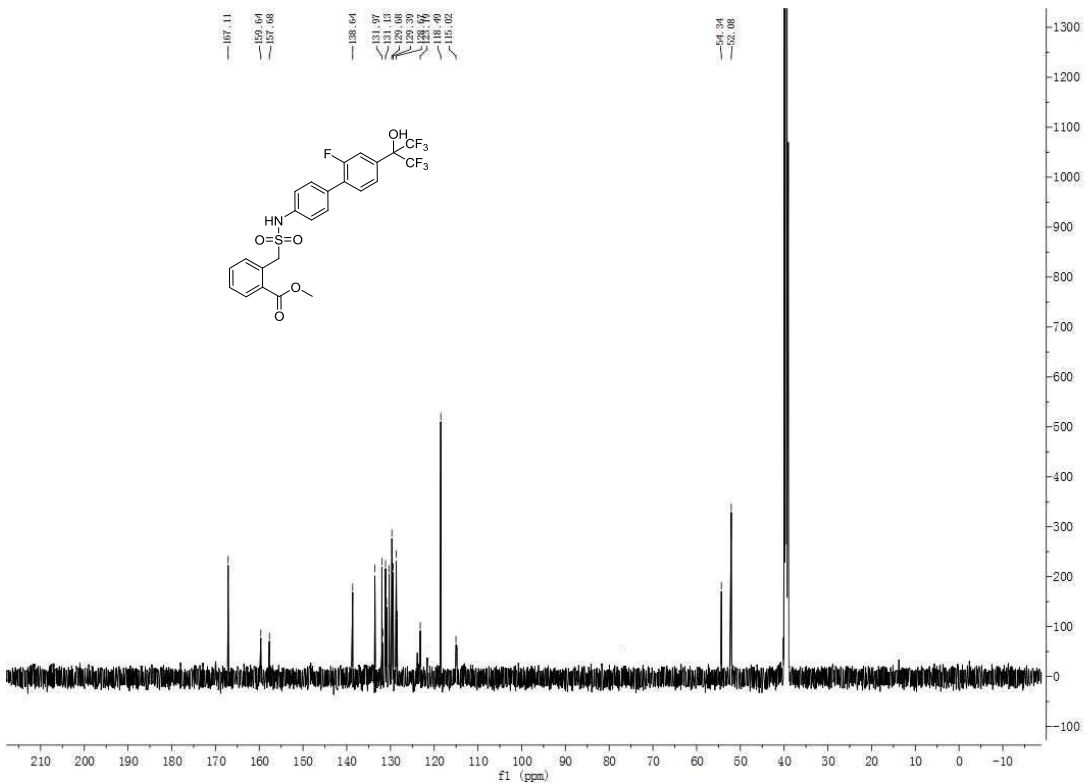
Methyl-3-((N-(2'-fluoro-4'-(1,1,1,3,3,3-hexafluoro-2-hydroxypropan-2-yl)-[1,1'-biphenyl]-4-yl)sulfamoyl)methyl)benzoate (20).



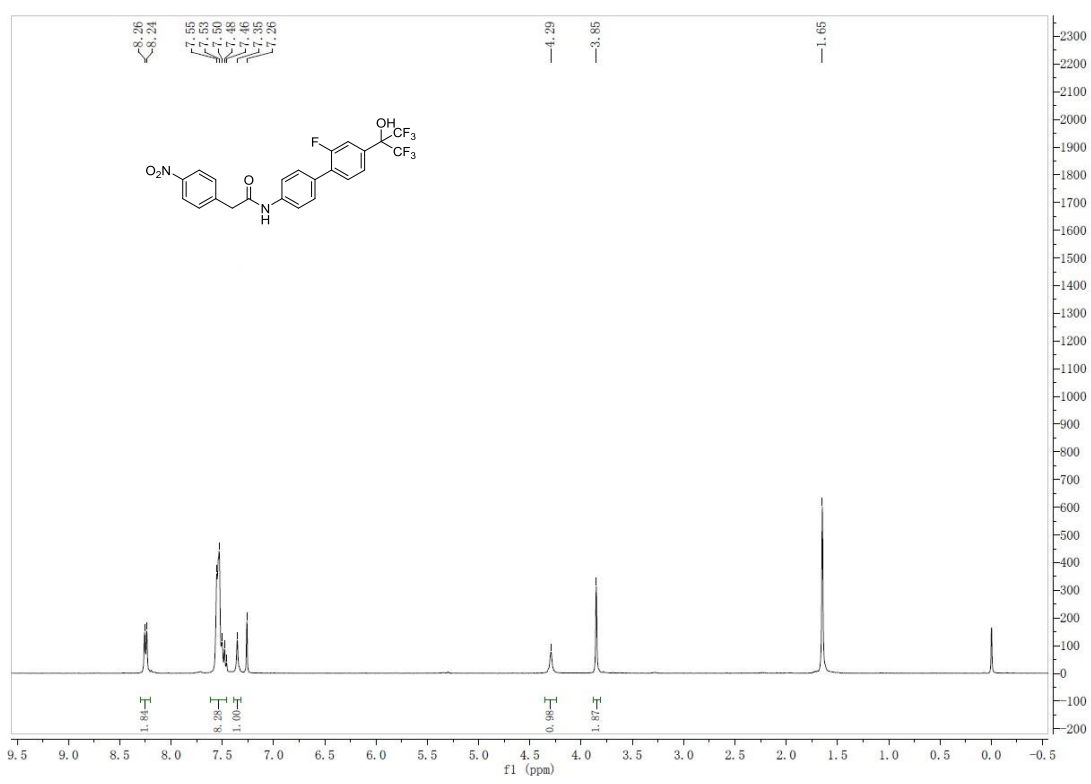


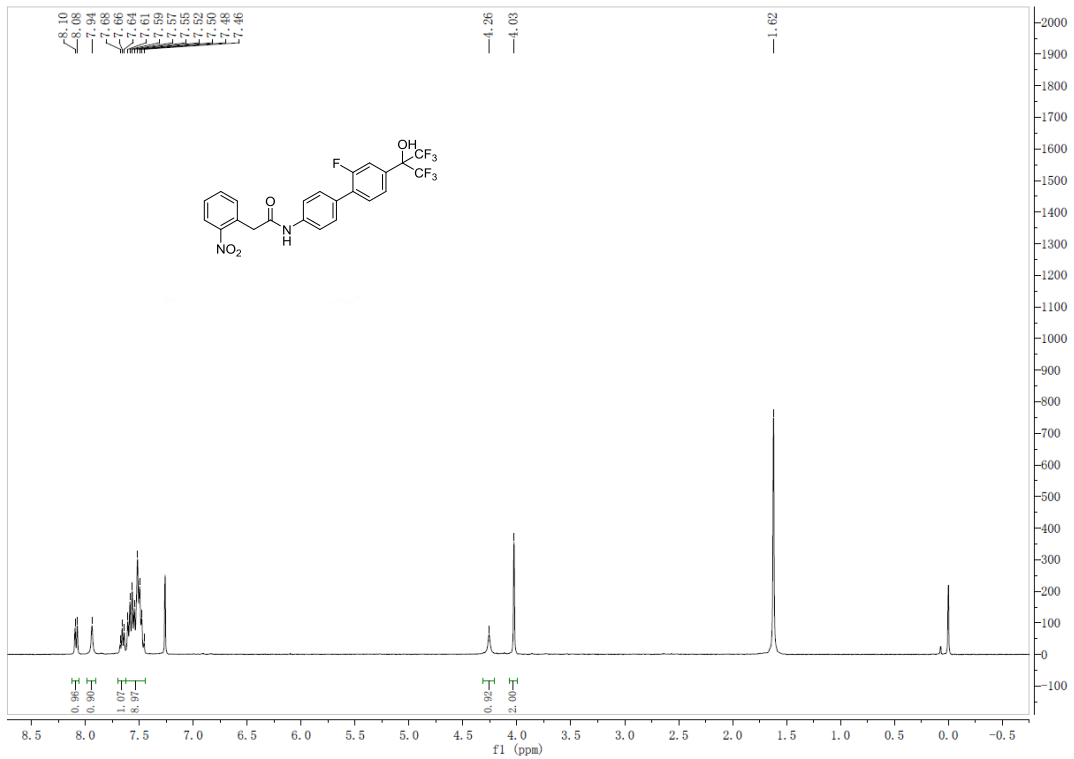
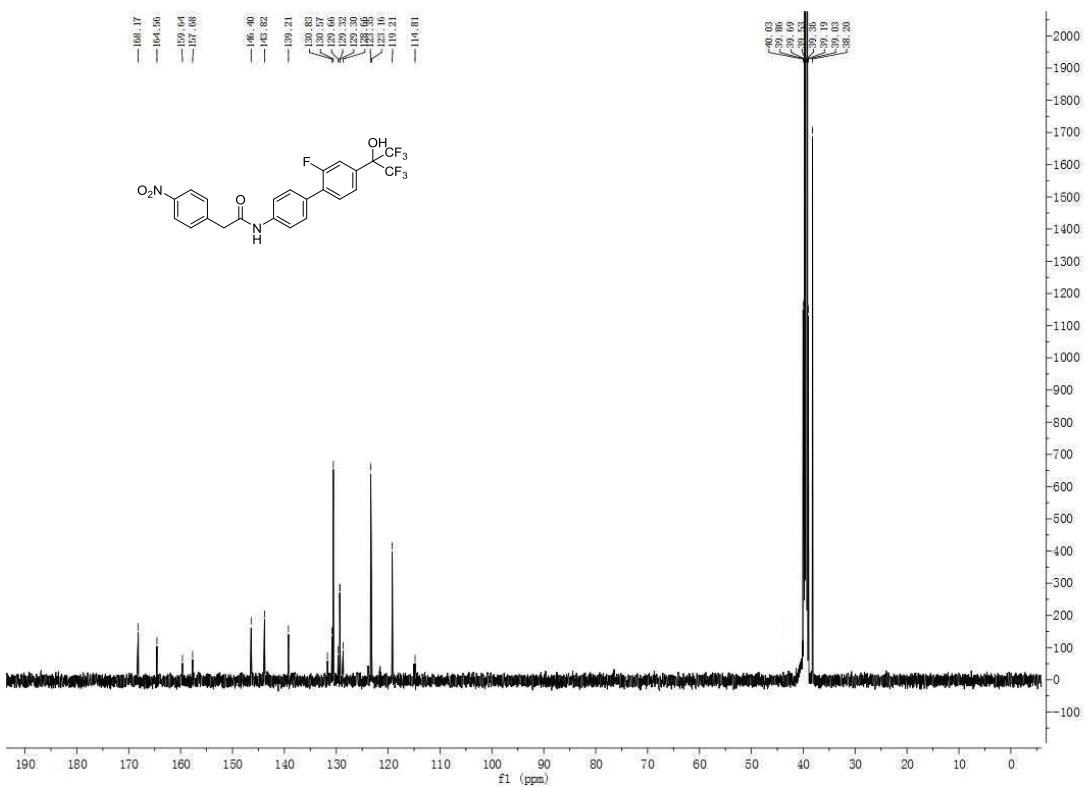
Methyl-2-((N-(2'-fluoro-4'-(1,1,1,3,3,3-hexafluoro-2-hydroxypropan-2-yl)-[1,1'-biphenyl]-4-yl)sulfonyl)methyl)benzoate (21)

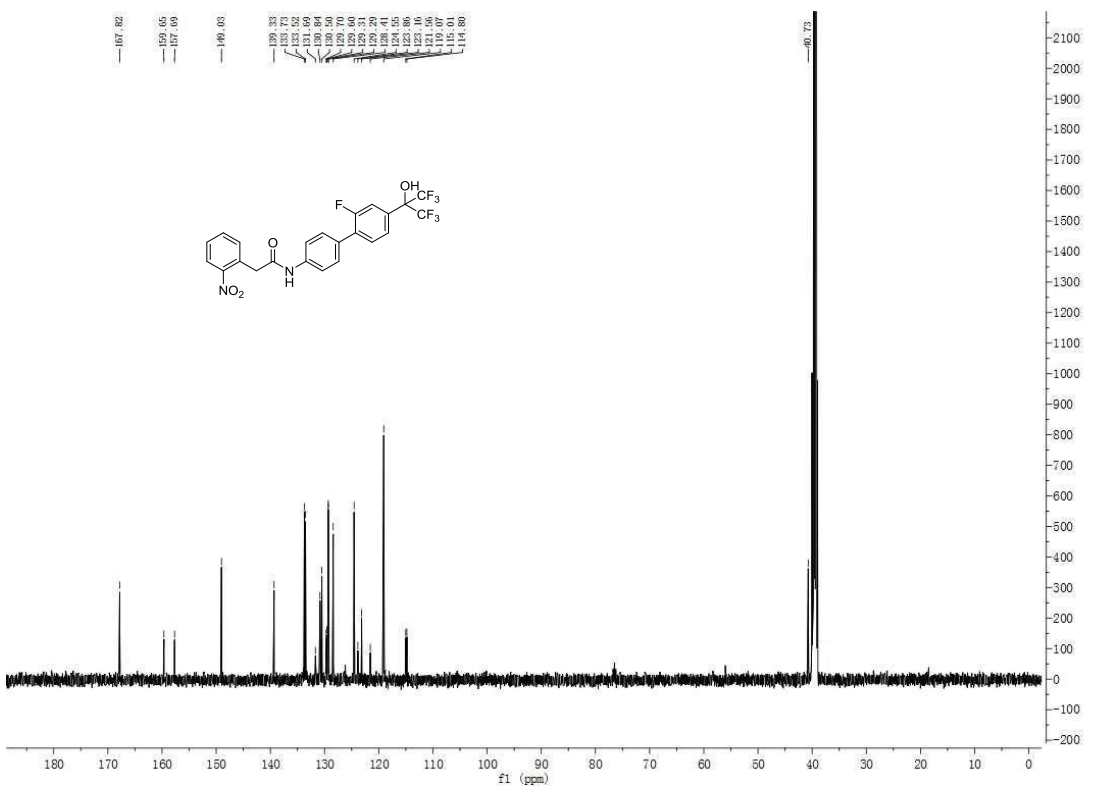




N-(2'-fluoro-4'-(1,1,1,3,3,3-hexafluoro-2-hydroxypropan-2-yl)-[1,1'-biphenyl]-4-yl)-2-(4-nitrophenyl)acetamide (**22**).

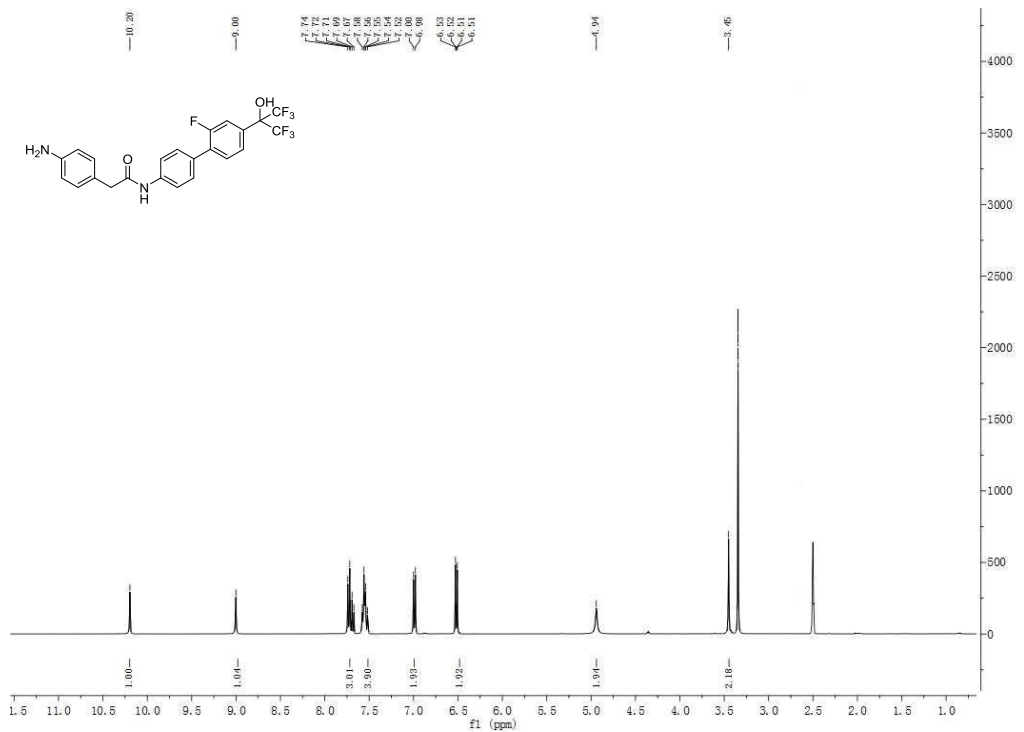




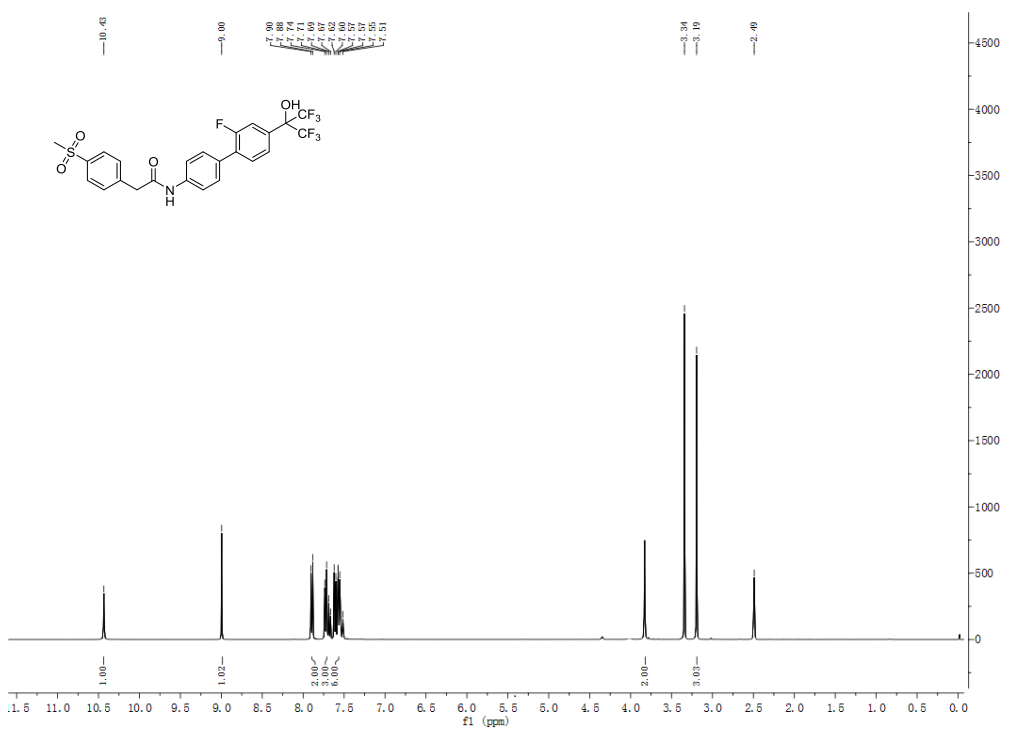
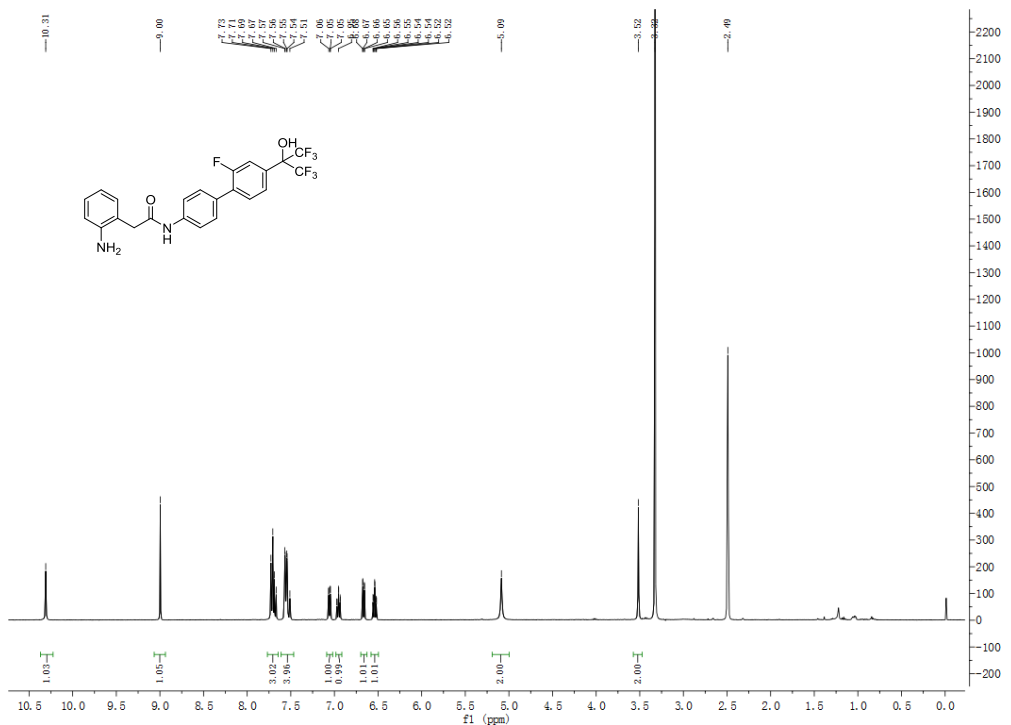


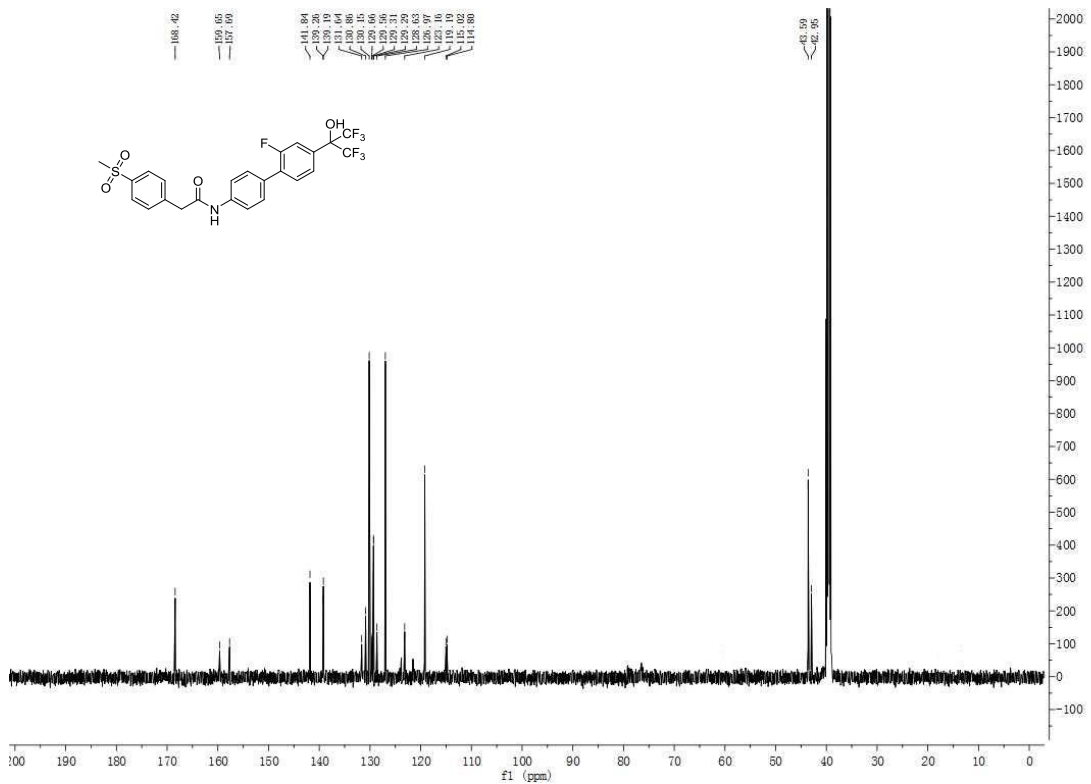
2-(4-nitrophenyl)-N-(2'-fluoro-4'-(1,1,1,3,3-hexafluoro-2-hydroxypropan-2-yl)-[1,1'-biphenyl]-4-yl)acetamide (**24l**).

4-yl)acetamide (24**).**

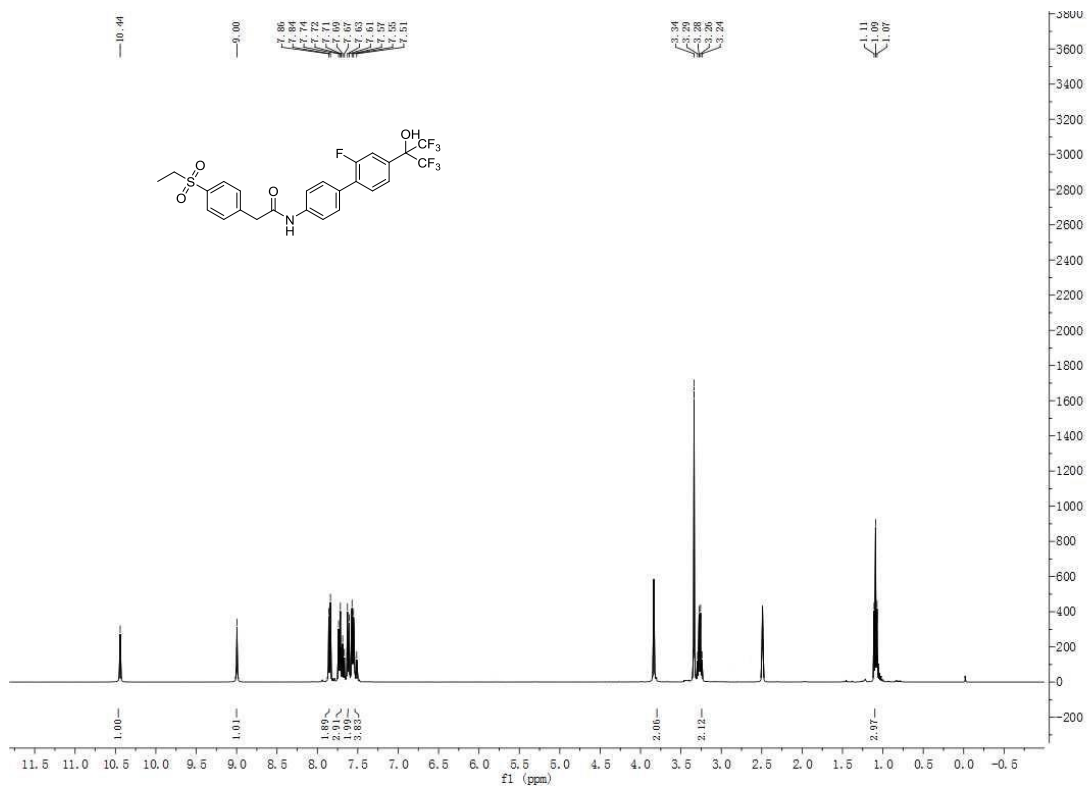


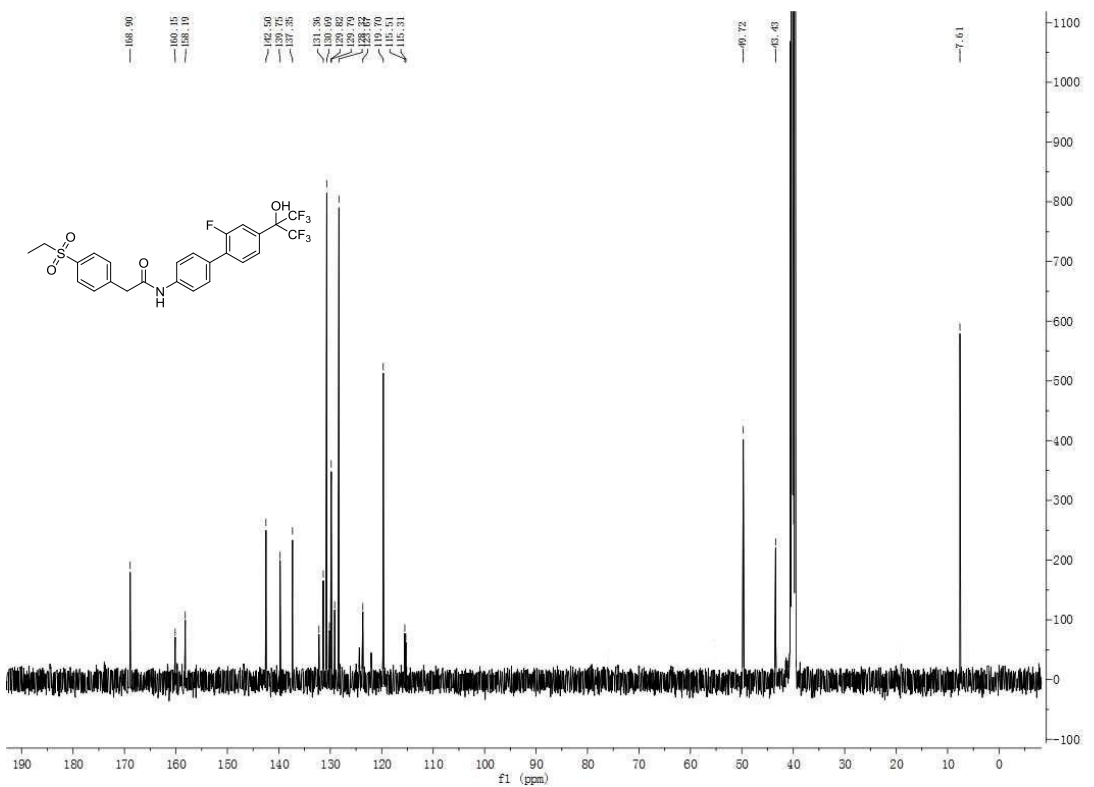
2-(2-aminophenyl)-N-(2'-fluoro-4'-(1,1,1,3,3-hexafluoro-2-hydroxypropan-2-yl)-[1,1'-biphenyl]-4-yl)acetamide (25).





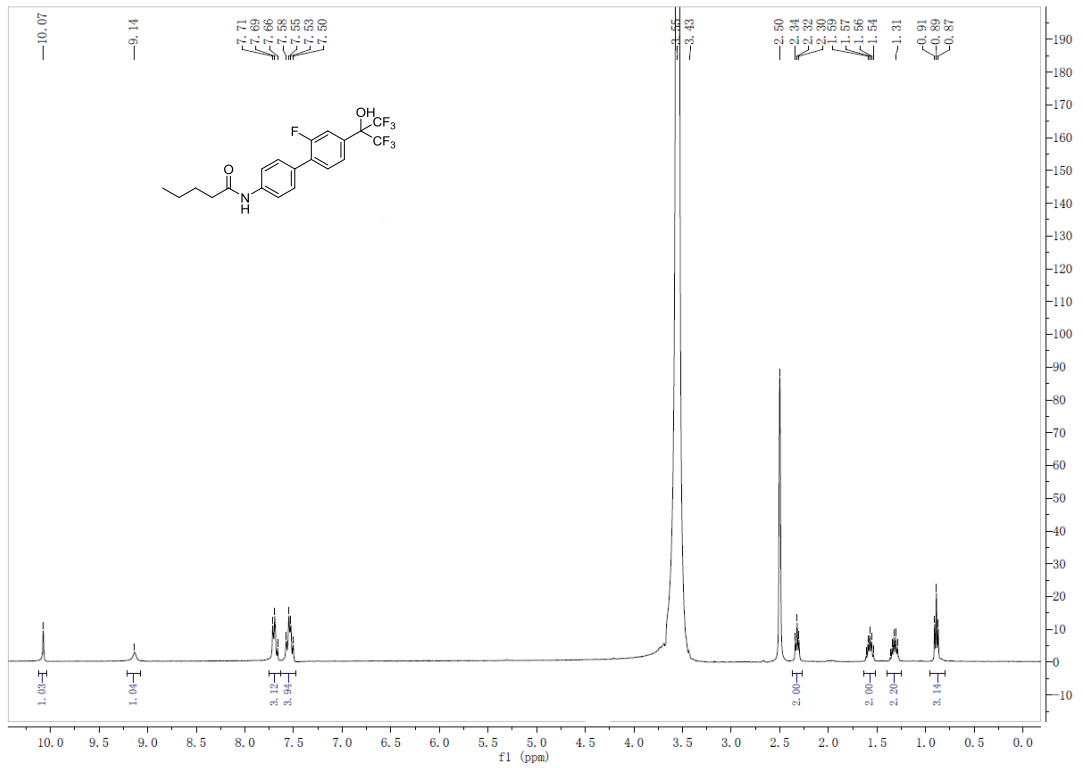
2-(4-(ethylsulfonyl)phenyl)-N-(2'-fluoro-4'-(1,1,1,3,3-hexafluoro-2-hydroxypropan-2-yl)-[1,1'-biphenyl]-4-yl)acetamide (27).

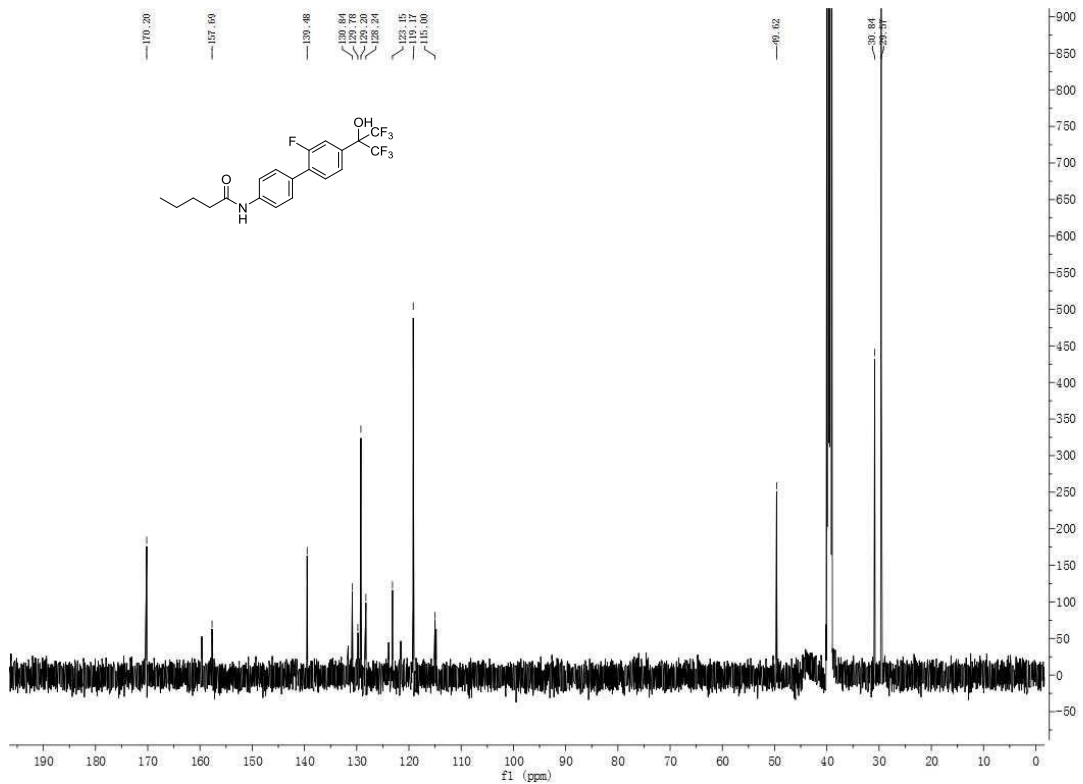




N-(2'-fluoro-4'-(1,1,1,3,3-hexafluoro-2-hydroxypropan-2-yl)-[1,1'-biphenyl]-4-yl)pentanamide

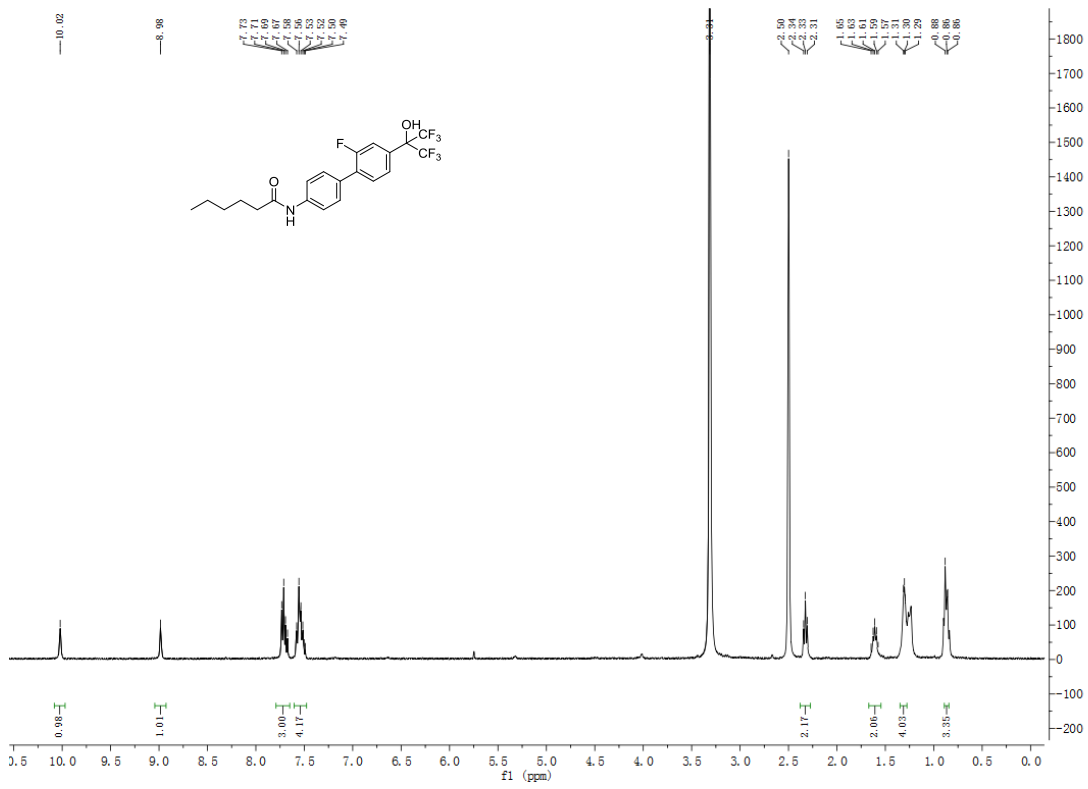
(28).

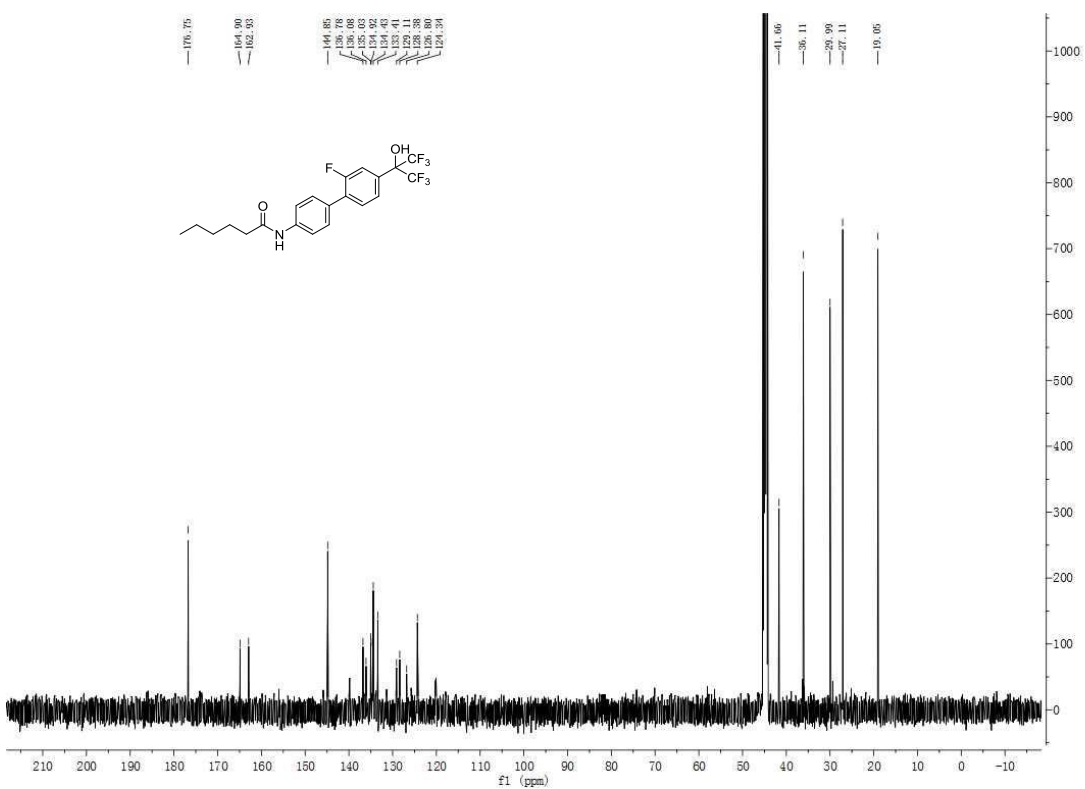




N-(2'-fluoro-4'-(1,1,1,3,3,3-hexafluoro-2-hydroxypropan-2-yl)-[1,1'-biphenyl]-4-yl)hexanamide

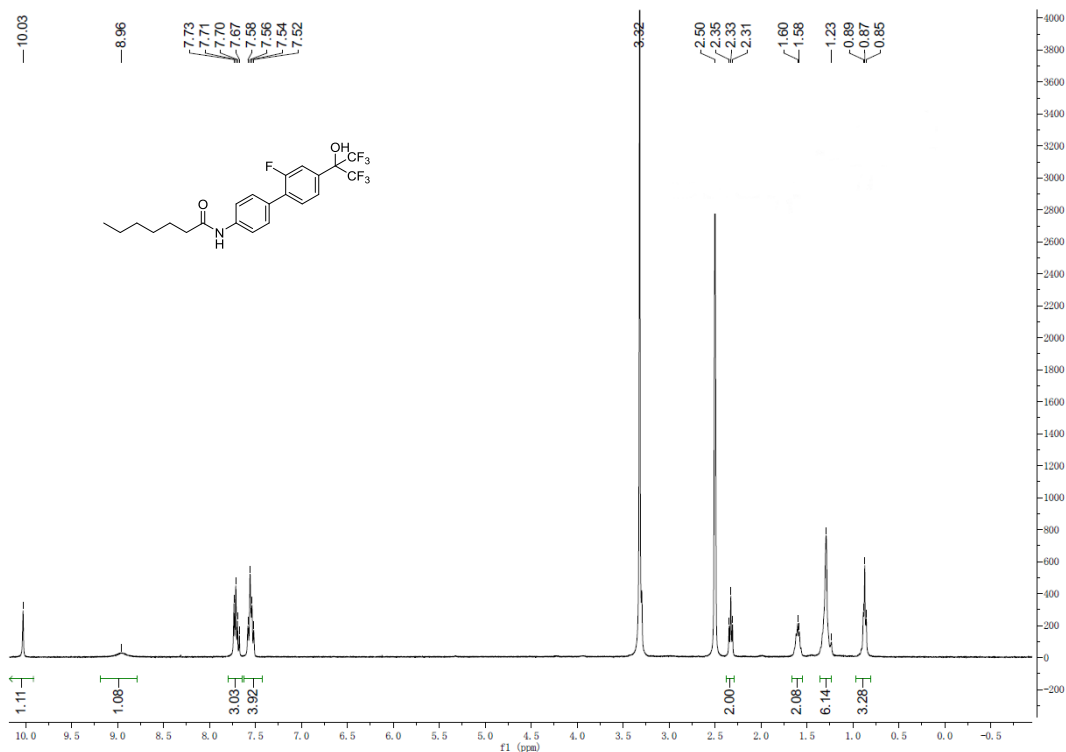
(29).

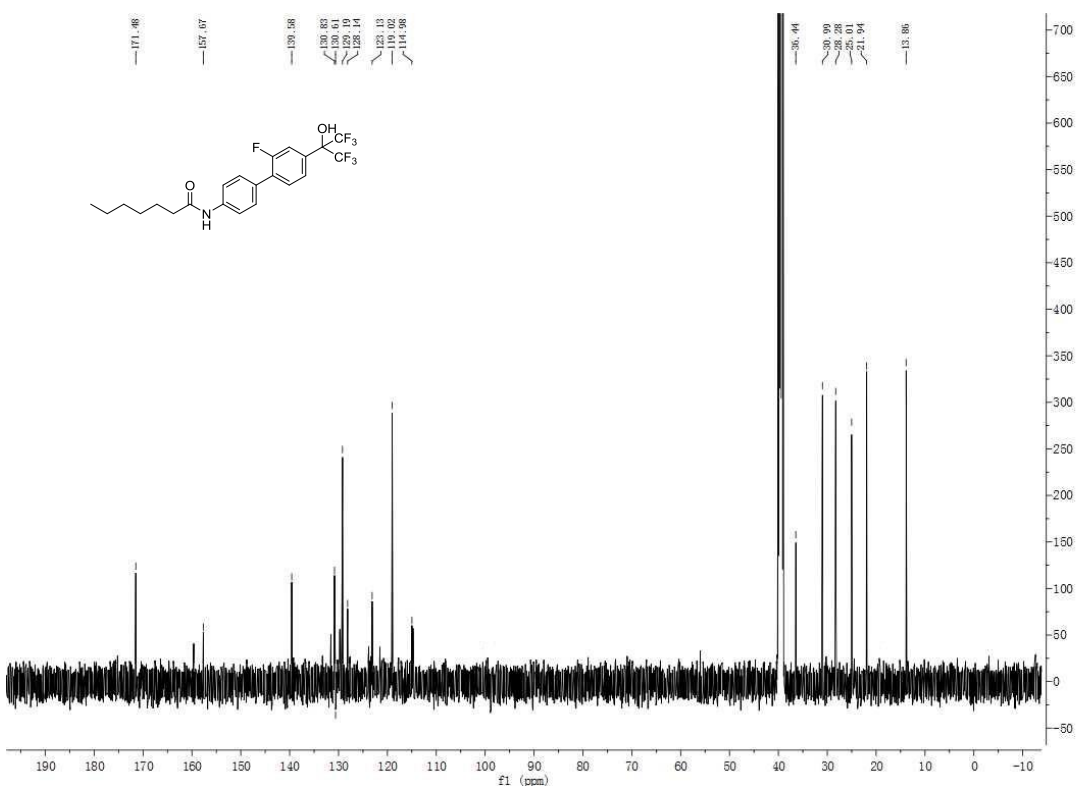




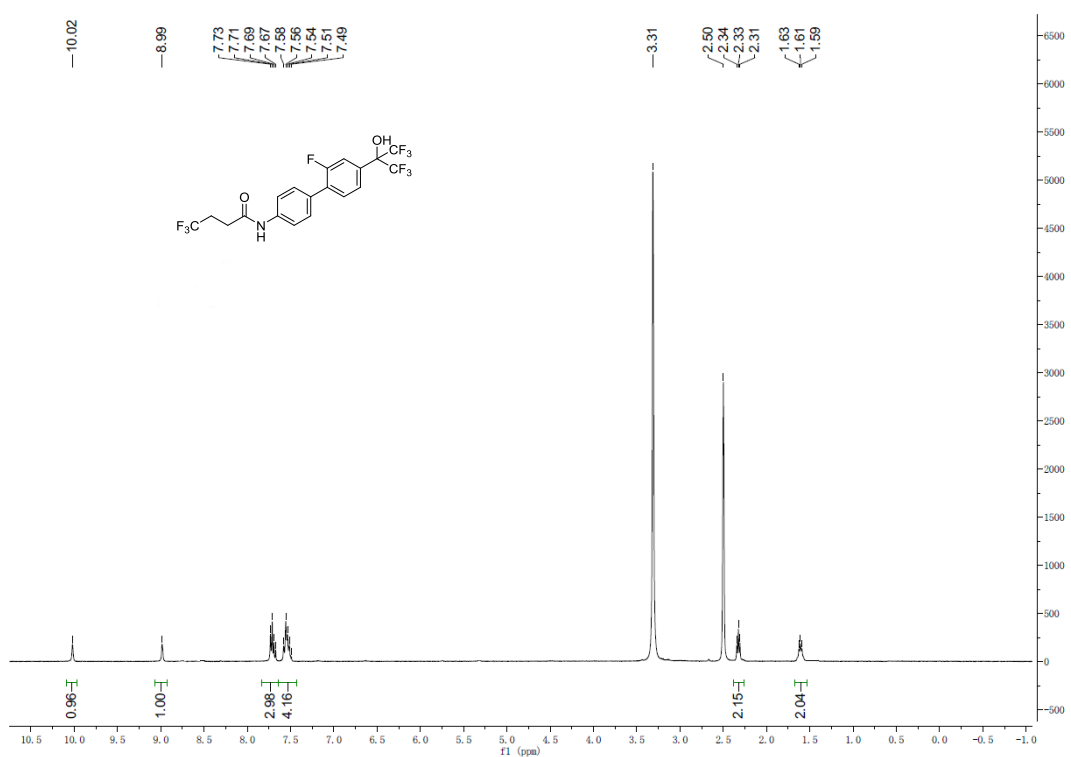
N-(2'-fluoro-4'-(1,1,1,3,3-hexafluoro-2-hydroxypropan-2-yl)-[1,1'-biphenyl]-4-yl)heptanamide

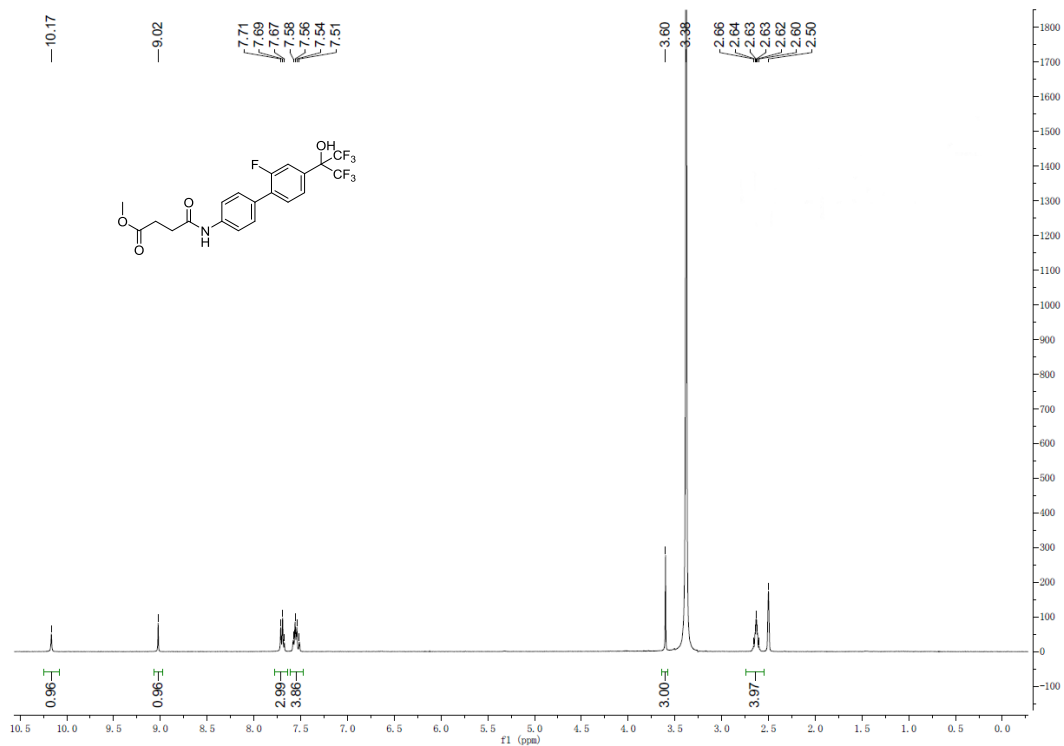
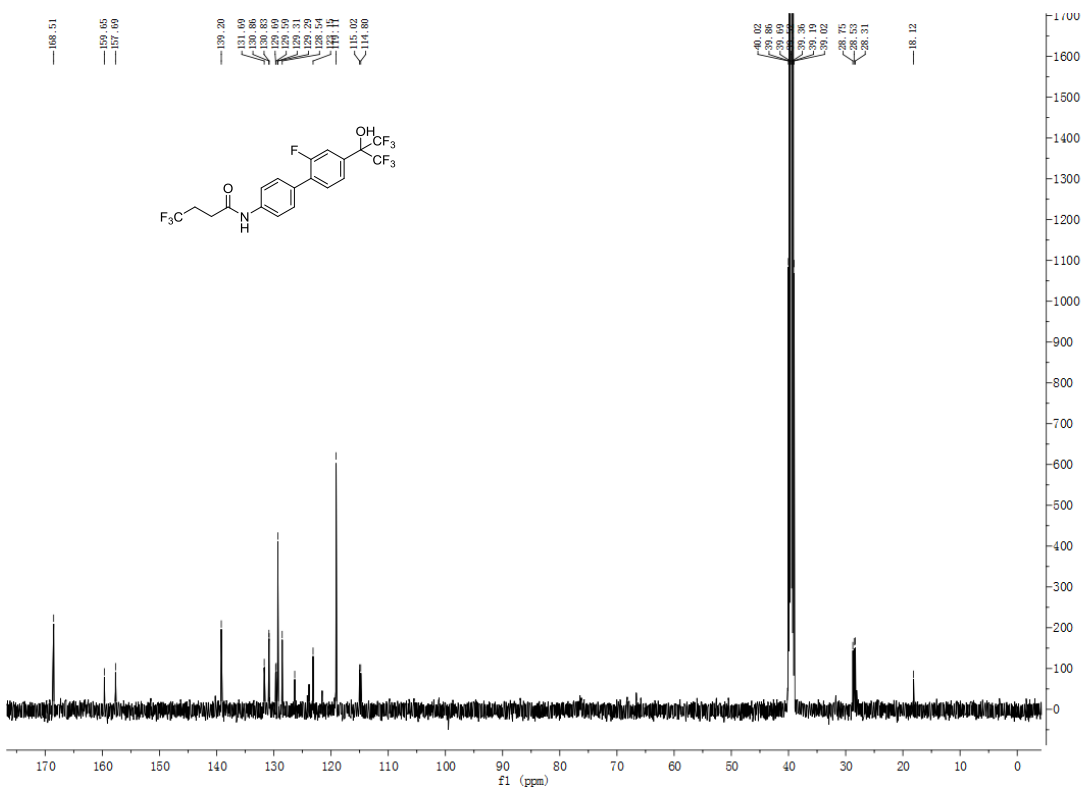
(30).

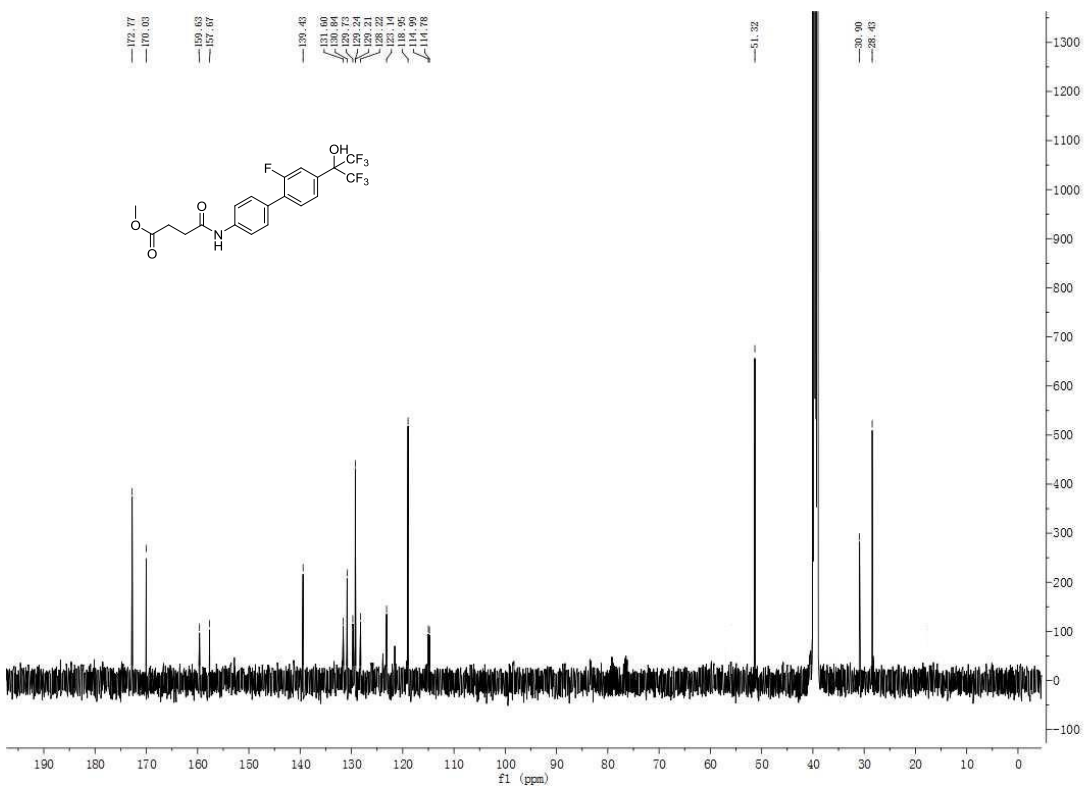




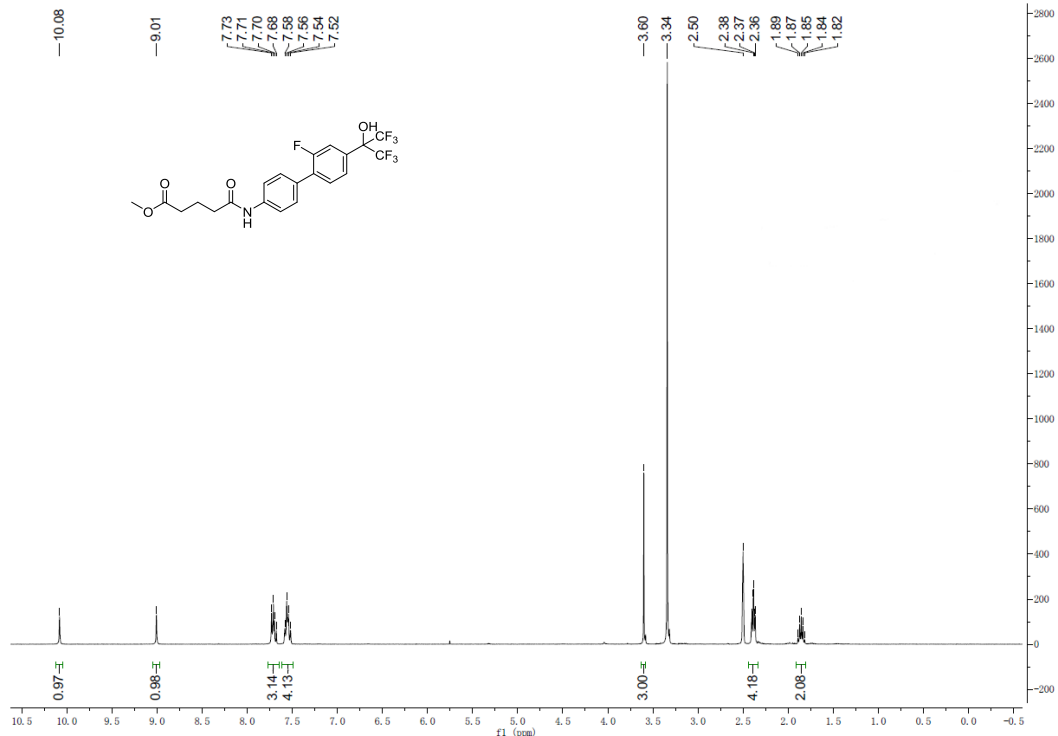
4,4,4-trifluoro-N-(2'-fluoro-4'-(1,1,1,3,3,3-hexafluoro-2-hydroxypropan-2-yl)-[1,1'-biphenyl]-4-yl)butanamide (31).

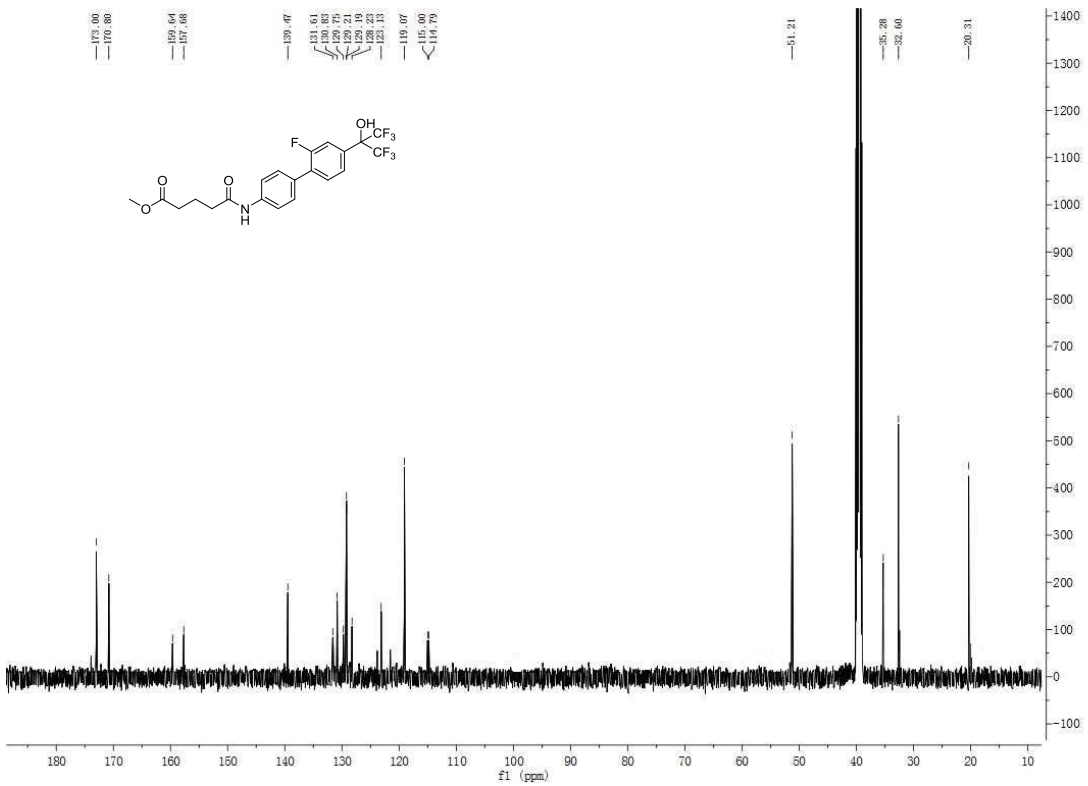




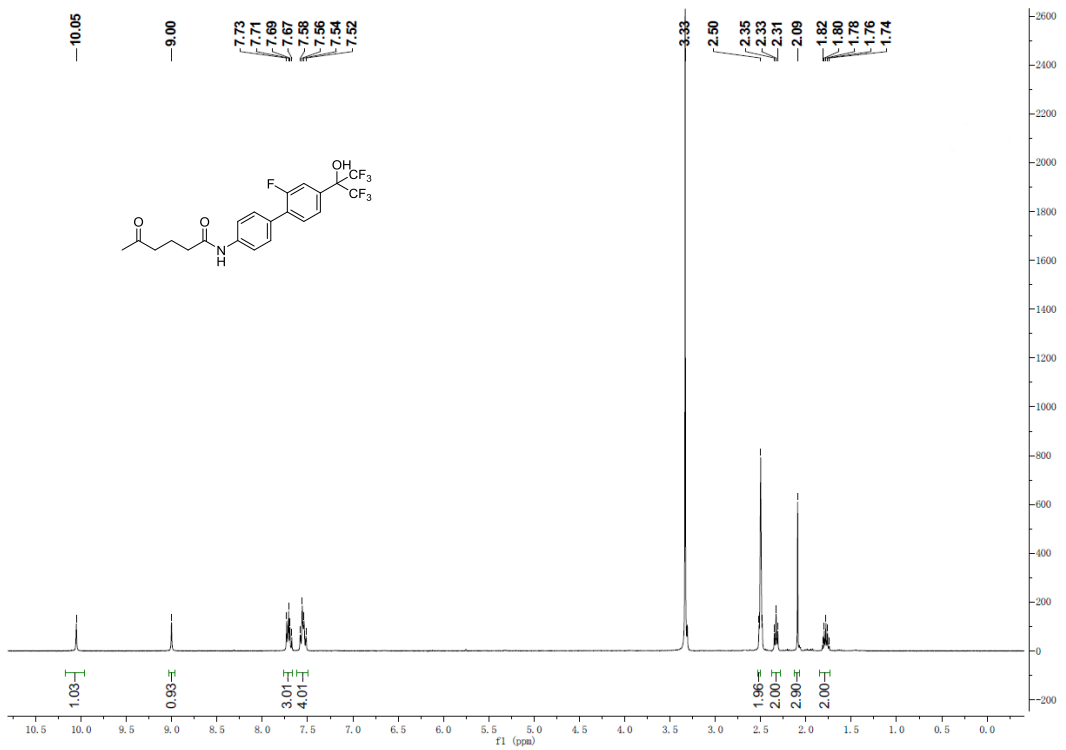


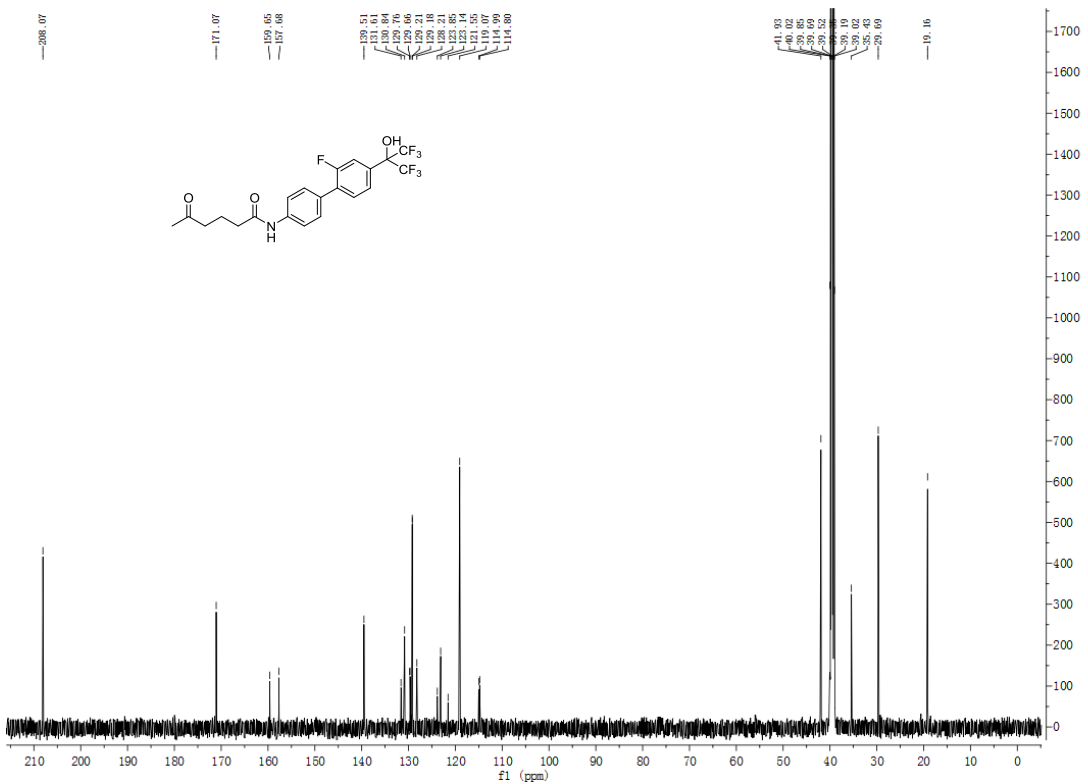
Methyl-5-((2'-fluoro-4'-(1,1,3,3,3-hexafluoro-2-hydroxypropan-2-yl)-[1,1'-biphenyl]-4-yl)amino)-5-oxopentanoate (33).



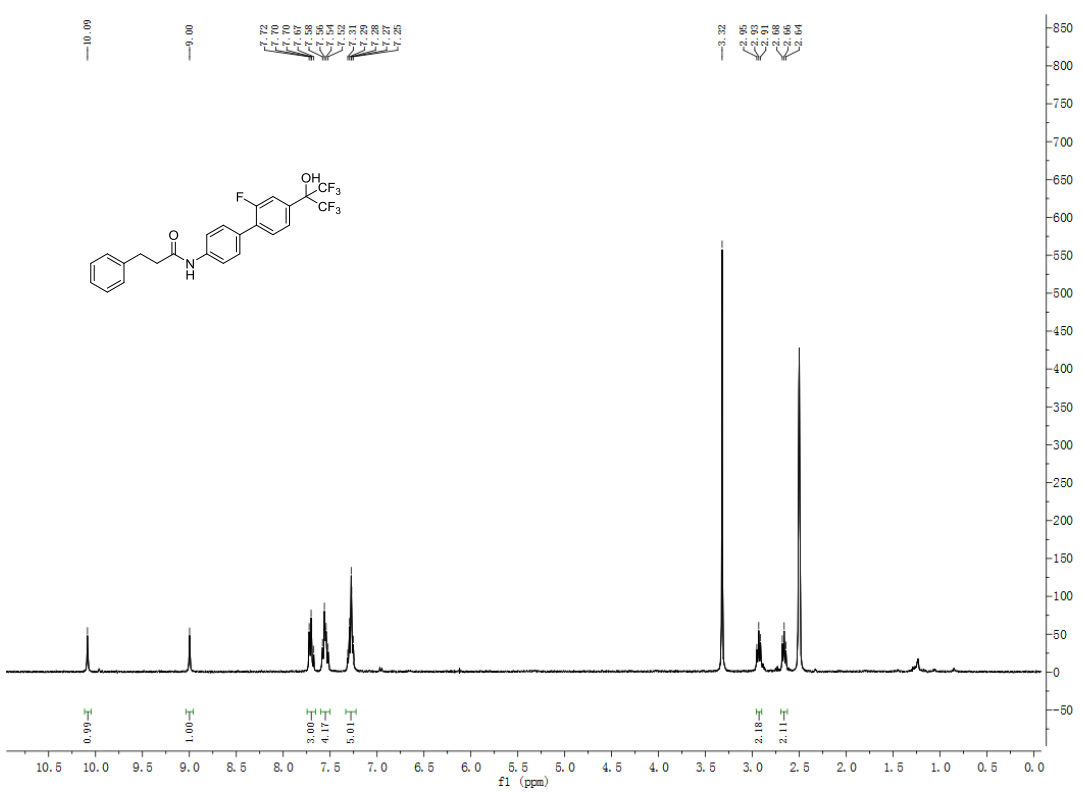


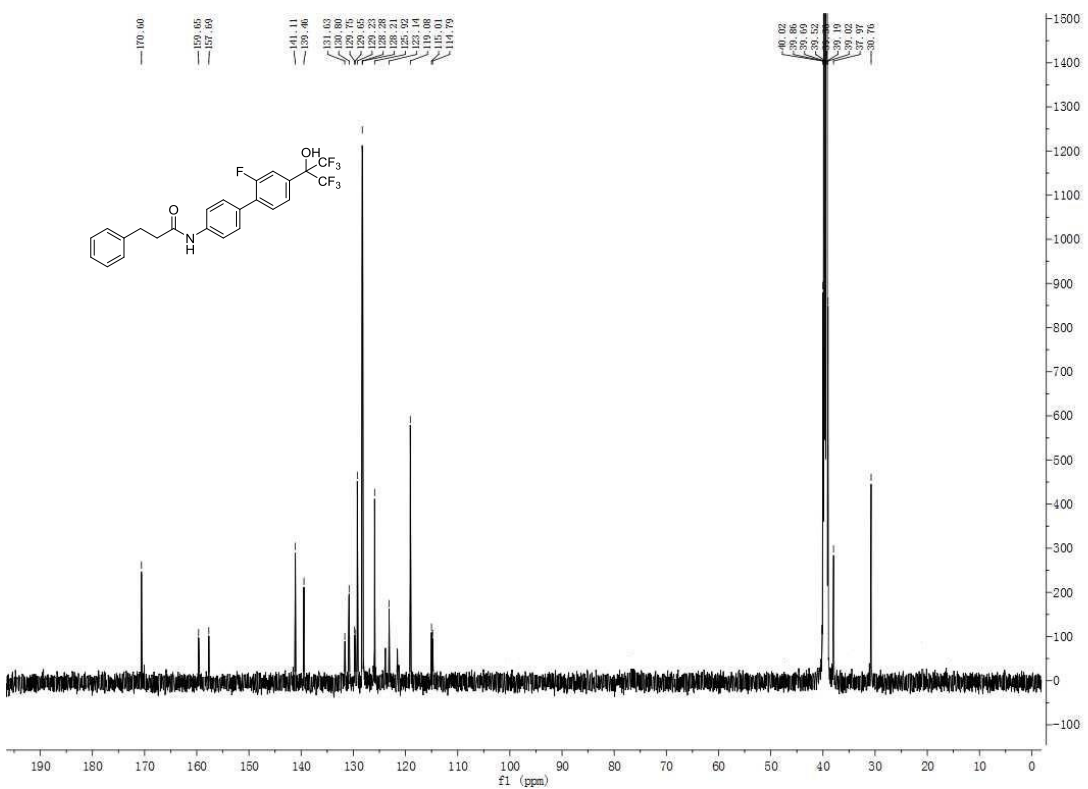
N-(2'-fluoro-4'-(1,1,3,3,3-hexafluoro-2-hydroxypropan-2-yl)-[1,1'-biphenyl]-4-yl)-5-oxohexanamide (**34**).





N-(2'-fluoro-4'-(1,1,1,3,3,3-hexafluoro-2-hydroxypropan-2-yl)-[1,1'-biphenyl]-4-yl)-3-phenylpropamide (35).





4-cyclohexyl-N-(2'-fluoro-4'-(1,1,1,3,3-hexafluoro-2-hydroxypropan-2-yl)-[1,1'-biphenyl]-4-yl)butanamide (36).

